

AN OPTIMAL FACTORIZATION PRECONDITIONER FOR PERIODIC SCHRÖDINGER EIGENSTATES IN ANISOTROPICALLY EXPANDING DOMAINS*

BENJAMIN STAMM[†] AND LAMBERT THEISEN[‡]

Abstract. This paper provides a provably optimal preconditioning strategy of the linear Schrödinger eigenvalue problem with periodic potentials for a possibly non-uniform spatial expansion of the domain. The optimality is achieved by having the iterative eigenvalue algorithms converge in a constant number of iterations with respect to different domain sizes. In the analysis, we derive an analytic factorization of the spectrum and asymptotically describe it using concepts from the homogenization theory. This decomposition allows us to express the eigenpair as an easy-to-calculate cell problem solution combined with an asymptotically vanishing remainder. We then prove that the easy-to-calculate limit eigenvalue can be used in a shift-and-invert preconditioning strategy to uniformly bound the number of eigensolver iterations. Several numerical examples illustrate the effectiveness of this optimal preconditioning strategy.

Key words. Periodic Schrödinger Equation, Asymptotic Eigenvalue Analysis, Factorization Principle, Preconditioner, Iterative Eigenvalue Solvers, Directional Homogenization

AMS subject classifications. 65N25, 65F15, 65N30, 35B27, 35B40

1. Introduction. In this paper, we consider the spectral problem for linear time-independent Schrödinger-type operators. Let us consider a parametrized family of d -dimensional boxes Ω_L given by

$$(1.1) \quad \mathbf{z} \in \Omega_L = (0, L)^p \times (0, \ell)^q = \Omega_{\mathbf{x}} \times \Omega_{\mathbf{y}} \subset \mathbb{R}^d,$$

with coordinates $\mathbf{z} := (\mathbf{x}, \mathbf{y}) = (x_1, \dots, x_p, y_1, \dots, y_q)$ and dimensions $L \in \mathbb{N}, \ell \in \mathbb{R}$. Note that we provide an extension to arbitrary domains in [subsection 4.3](#) and only keep the box shape for the early chapters of the analysis. We denote by $H_0^1(\Omega_L)$ the standard Sobolev space of index 1 with zero Dirichlet trace on Ω_L .

Then we consider the eigenvalue problem: Find $(\phi_L, \lambda_L) \in (H_0^1(\Omega_L) \setminus \{0\}) \times \mathbb{R}$, such that

$$(1.2) \quad -\Delta \phi_L + V \phi_L = \lambda_L \phi_L \quad \text{in } \Omega_L.$$

Here, ϕ_L and λ_L are the eigenfunctions and -values, respectively, while the function V encodes an external potential applied to the system. Typically, we are interested in the computation of some of the smallest eigenpairs of [\(1.2\)](#).

For the analysis, we make the following assumptions for the potential:

- (A1) The potential V is directional-periodic with a period of 1 in each expanding direction: $V(\mathbf{x}, \mathbf{y}) = V(\mathbf{x} + \mathbf{i}, \mathbf{y}) \quad \forall (\mathbf{x}, \mathbf{y}) \in \Omega_L, \mathbf{i} \in \mathbb{Z}^p$;
- (A2) The potential V is essentially bounded: $V \in L^\infty(\Omega_L)$;
- (A3) The potential V is non-negative: $V \geq 0$ a.e. in Ω_L .

Note that under the assumption (A2), we can always apply a constant spectral shift to the potential without affecting the eigenfunctions to fulfill (A3). Of course,

* \LaTeX compiled on October 29, 2021.

Funding: This work was supported by the German Research Foundation (DFG) under project 411724963.

[†] Applied and Computational Mathematics, RWTH Aachen University, 52062 Aachen, Germany (best@acom.rwth-aachen.de).

[‡] Corresponding author. Applied and Computational Mathematics, RWTH Aachen University, 52062 Aachen, Germany (theisen@acom.rwth-aachen.de).

(A1) is only chosen for simplicity and arbitrary periods are possible. Furthermore, we could extend the theory to general elliptic operators satisfying the properties of [subsection 2.1](#). [Figure 1a](#) presents the geometrical framework.

We focus on the case of q fixed dimensions of length ℓ . In contrast, the other p dimensions expand with $L \rightarrow \infty$. This geometric setup allows us to study chain-like ($d = 2, p = 1$) or plane-like ($d = 3, p = 2$) domains with $L \rightarrow \infty$. These are the most common application cases. However, the setup is not limited to $d \leq 3$, and all results also hold in the general case.

Suppose one aims to solve for the ground-state eigenpair (smallest eigenvalue). In that case, the convergence rate of typical numerical algorithms [[22](#), p53] depends on the fundamental ratio between the first and the second ($\lambda_L^{(1)} < \lambda_L^{(2)}$) eigenvalue

$$(1.3) \quad r_L := |\lambda_L^{(1)}|/|\lambda_L^{(2)}| \leq 1.$$

Our geometrical setup of Ω_L , with $(0, L)^p \rightarrow (0, \infty)^p$ and $(0, \ell)^q$ being fix can lead to a collapsing fundamental gap $\lambda_L^{(1)} - \lambda_L^{(2)} \rightarrow 0$ and thus $r_L \rightarrow 1$ as $L \rightarrow \infty$. This will deteriorate the convergence rate in the limit. Therefore, the eigensolver routine needs more and more iterations to converge to a fixed tolerance as L increases. To overcome this problem, we theoretically study the operator's spectrum in [\(1.2\)](#) to construct a suitable shift-and-invert preconditioner, such that the preconditioned fundamental gap $r_L(\sigma) := |\lambda_L^{(1)} - \sigma|/|\lambda_L^{(2)} - \sigma|$ is uniformly bounded above by a constant $C < 1$, for some $L > L^*$. For this strategy to work, we need to choose a shift σ based on the asymptotic behavior of the problem. As it turns out later, the optimal shift σ has to be the asymptotic eigenvalue $\lambda_\infty := \lim_{L \rightarrow \infty} \lambda_L^{(1)}$.

1.1. Motivation: Collapsing Fundamental Gap for the Laplace Eigenvalue Problem. Even for the simplest potential satisfying the assumptions (A1)–(A3), namely $V(\mathbf{z}) = 0$, the fundamental gap r_L decreases if only a subset of directions in Ω_L is increased. The simplicity of the Laplace eigenvalue problem allows us to highlight the main challenges by considering the explicitly known eigenvalues. For $p = 1$ and $q = 1$, the pure Laplace eigenvalue problem has eigenvalues $\lambda_L^{(1)} = \pi^2/L^2 + \pi^2/\ell^2$, $\lambda_L^{(2)} = 4\pi^2/L^2 + \pi^2/\ell^2$. It is then evident that $\lim_{L \rightarrow \infty} \lambda_L^{(1)}/\lambda_L^{(2)} = 1$ for $L \rightarrow \infty$. Thus, this leads to a decreasing converge rate r_L . In the eigenvalue lattice illustrated in [Figure 1b](#), the collapsing fundamental gap is visible. In such a representation, each point represents an eigenvalue $\lambda_L^{(m)}$, and its distance to the origin corresponds to $\sqrt{\lambda_L^{(m)}/\pi}$. All eigenvalues will form continuous x -parallel lines for the asymptotic case of $L \rightarrow \infty$. For this Laplace eigenvalue problem, a shift of $\sigma = \lambda_\infty = \pi^2/\ell^2$ would lead to $\lim_{L \rightarrow \infty} r_L(\sigma) = 1/4 < 1$.

This simple example serves as a motivation. However, to give a systematic approach to choosing the asymptotic correct shift σ in the general case, we develop a framework on characterizing the asymptotic behavior of the spectral properties for Schrödinger operators with periodic potentials satisfying (A1)–(A3). Knowing the asymptotic behavior will allow solving the algebraic eigenvalue problem within only a constant number of eigensolver iterations.

1.2. State-of-the-Art and Context. We can embed our results to existing research for three different aspects – the considered model equation itself, the geometrical setup with the present periodic potential, and other mathematical analyses for related equations.

First, the Schrödinger equation [\(1.2\)](#) describes the stationary states of the wave

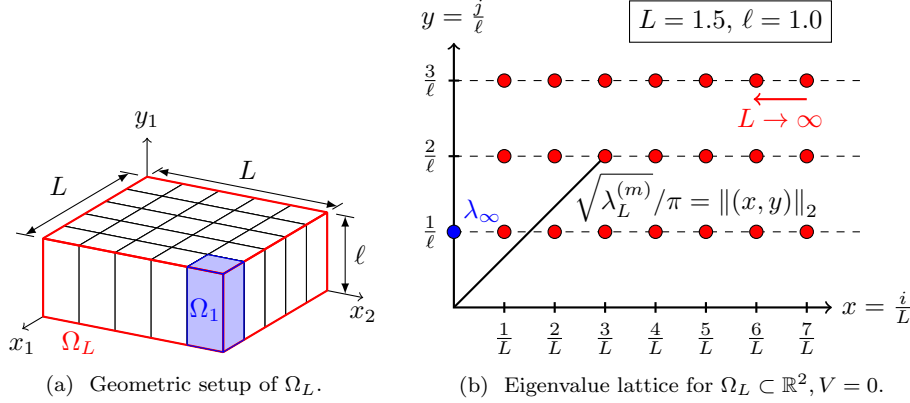


FIG. 1. *Figure 1a: Geometric setup with $p = 2$ expanding directions with length L and $q = 1$ fixed dimensions with length ℓ . Figure 1b: The spectrum of the Dirichlet Laplacian on a rectangle domain $\Omega_L = (0, L) \times (0, \ell)$ mapped to an eigenvalue lattice.*

function ϕ_L for a quantum-mechanical system influenced by an external potential V . Therefore, example applications naturally arise in computational chemistry and quantum mechanics in general. Since the present model is one of the simpler models, it is only suitable for the direct simulation of basic quantum systems. In more elaborate electronic structure calculations, a nonlinear version of the Schrödinger equation is used. However, there is always a need to solve systems similar to (1.2) in self-consistent field (SCF) iterations [42, 25, 45] or other types of iteration schemes to solve these nonlinear Schrödinger-type equations [17, 18, 19]. One of such examples is the Bose–Einstein condensate, either modeled with random or disorder potentials [16, 14] or modeled with the Gross–Pitaevskii eigenvalue problem [15, 13, 14, 43]. Other applications for the same equation (1.2) arise in studying the power distribution in a nuclear reactor core [6, 9, 39].

Second, when it comes to the geometric setup of only a subset of dimensions expanding, applications arise, for example, in material science to study the electronic properties of plane-like, layered [27, 26] or chain-like structures, such as carbon nanotubes [1] or polymers chains [58].

Third, from a mathematical point of view, the study of elliptic operators in the context of source problems with homogenization [38, 37, 53, 35, 32, 29, 31] is closely related since V is periodic (at least directional in our setup). Also, for eigenvalue problems with periodic coefficients, results in [34, 30, 33] show the presence of asymptotic limit solution when the domain expands in some directions to infinity. Finally, from a technical point of view, our analysis in section 2 extends aspects of the work by Allaire et al. in [7, 6, 11, 5, 9, 8]. Especially the concept of factorization will be one of the main techniques in our analysis. It allows us to analytically describe the spectrum of the system in terms of easier cell problems. This idea traces back to [56, 47, 48].

1.3. Contribution and Main Results. This work aims to provide a numerical framework to solve the eigenvalue problem (1.2) in a fixed number of eigensolver iterations for all domain sizes $L \rightarrow \infty$. We, therefore, propose a shift-and-invert strategy with an optimally chosen shift. The theoretical derivation of this particular shift is based on the following factorization of the eigenfunctions (see Theorem 2.5 for

a more precise statement)

$$(1.4) \quad \phi_L^{(m)} = \psi \cdot u_{y,1} \cdot u_{y,2}^{(m)} = \varphi_y \cdot u_{y,2}^{(m)},$$

$$(1.5) \quad \lambda_L^{(m)} = \lambda_\psi + \lambda_{u_{y,1}} + \lambda_{u_{y,2}}^{(m)} = \lambda_{\varphi_y} + \lambda_{u_{y,2}}^{(m)} = \lambda_{\varphi_y} + \mathcal{O}(1/L^2).$$

The above characterization highlights that we can simply use λ_{φ_y} as the optimal shift since we will show that the remaining term $\lambda_{u_{y,2}}^{(m)}$ tends to zero as $L \rightarrow \infty$ for all m . In contrast to existing literature, this statement considers the case where only a subset of dimensions expands, and the periodicity is directional, which is essential given the potential practical applications. The eigenpair $(\varphi_y, \lambda_{\varphi_y})$ can be obtained in a constant time since it does not depend on $L \rightarrow \infty$ as it is a solution to a fixed-size spectral cell problem. We then show that this eigenpair is the asymptotic limit as

$$(1.6) \quad \lim_{L \rightarrow \infty} \lambda_L^{(m)} = \lambda_{\varphi_y}.$$

These results, then, directly imply that the preconditioned fundamental ratio r_L is uniformly bounded from above by a constant for all $L > L^*$, which is smaller than one (see [Theorem 2.9](#) for a more precise statement). Since the convergence speed of the iterative eigensolvers depends on precisely this ratio, they converge in a constant number of iterations, and our goal is achieved.

The main challenges arise in the analysis and the optimality proof of the preconditioner. The idea of using factorization results to construct an optimal preconditioner for an anisotropic domain size increase, which can be computed in $\mathcal{O}(1)$, is not covered, up to our knowledge, in the existing literature. Moreover, although the idea of factorization is not new (see the references in [subsection 1.2](#)), it was not yet applied in the context of weighted and thus potentially degenerate Sobolev spaces. However, precisely this setup of degenerate weights is necessary for our optimality analysis since the zero Dirichlet boundary conditions on the \mathbf{y} -boundary significantly contribute to the asymptotic behavior of the spectrum. In addition, proving optimality also requires bounding the fundamental ratio of the preconditioned system uniformly. Thus, another challenge is interpreting the expanding problem as a homogenization problem in a degenerate situation. This observation allows us to explicitly determine the asymptotic behavior of the m -dependent contribution in [\(1.4\)](#) and [\(1.5\)](#). However, unlike the classical homogenization theory, our homogenized limit is purely determined by an p - rather than an $(p+q)$ -dimensional problem, which seems to be a unique specialty of anisotropic expansion problems.

1.4. Outline. In [section 2](#), we present the theoretical framework for the factorization approach in [subsection 2.2](#), which allows us to consider the remaining simplified problems using the theory of homogenization in [subsection 2.3](#) to derive optimality statements. We then discretize and solve the eigensystem in [section 3](#) and show that the theoretical results also hold when specific subspace properties are met in the discrete setting. Next, [section 4](#) presents various numerical examples and shows the relevance of the method to solve practical problems. Finally, we conclude with some remarks and point out future work in [section 5](#).

2. Factorization and Homogenization of the Model Problem. In this chapter, we will use factorization and homogenization to derive the asymptotic spectrum, which allows us to specify the limit eigenvalue $\lambda_{\varphi_y} = \lim_{L \rightarrow \infty} \lambda_L^{(m)}$.

2.1. Existence and Regularity Results. The second-order partial differential operator in (1.2) is self-adjoint (by the symmetry of the diffusion matrix δ_{ij}), is positive-definite (by ellipticity/coercivity of the Laplacian plus a non-negative potential), and has bounded coefficients (since $V \in L^\infty(\Omega_L)$). We can therefore recall the classical existence results from [41, 56, 43] to establish well-posedness of our problem, that there exists a sequence $(m = 1, \dots, \infty)$ of eigenvalues with finite multiplicity $\lambda_L^{(m)}$ and a sequence of eigenfunctions $\phi_L^{(m)}$ (orthogonal basis of $H_0^1(\Omega_L)$) such that $0 < \lambda_L^{(1)} < \lambda_L^{(2)} \leq \lambda_L^{(3)} \leq \dots \rightarrow \infty$ and $\phi_L^{(1)} > 0$ a.e. for $\mathbf{z} \in \Omega_L$.

2.2. Factorization of the Eigenfunctions and Eigenvalues. Our next step is to establish factorizations for the solution to the eigenvalue problem (1.2). Thus, we describe splitting an eigenfunction into a product of two or more functions and splitting an eigenvalue into the sum of two or more eigenvalues. This splitting can be seen as a generalization to the separation of variables for the pure Laplace case.

In the following, we will make use of multiple eigenvalue problems and their solutions. Therefore, we unify the notation and introduce the abstract notation:

DEFINITION 2.1 (Prototype of a Schrödinger eigenvalue problem). For $\Omega_L = (0, L)^p \times (0, \ell)^q \subset \mathbb{R}^d$, we define the m -th eigenpair

$$(2.1) \quad (u, \lambda)_{\mathcal{B}_x, \mathcal{B}_y, \rho, V}^{(m)} := \left(u_{\mathcal{B}_x, \mathcal{B}_y, \rho, V}^{(m)}(\Omega_L), \lambda_{\mathcal{B}_x, \mathcal{B}_y, \rho, V}^{(m)}(\Omega_L) \right),$$

to be the m -th eigenpair (including multiplicities) of the generalized Schrödinger-type eigenvalue problem: Find $(u, \lambda) \in (H_{\mathcal{B}_x, \mathcal{B}_y}^1(\Omega_L; \rho) \setminus \{0\}) \times \mathbb{R}$, such that

$$(2.2) \quad \begin{cases} -\nabla \cdot (\rho \nabla u) + Vu = \lambda \rho u & \text{in } \Omega_L, \\ \mathcal{B}_x(u) = 0 & \text{on } \partial(0, L)^p \times (0, \ell)^q, \\ \mathcal{B}_y(u) = 0 & \text{on } (0, L)^p \times \partial(0, \ell)^q, \end{cases}$$

with $0 \leq \rho, V \in L^\infty(\Omega_L)$, $1/\rho \in L_{loc}^1(\Omega_L)$, and $\mathcal{B}_x, \mathcal{B}_y \in \{\mathcal{B}_d, \mathcal{B}_n, \mathcal{B}_\#\}$ denoting the boundary operators

$$(2.3) \quad \text{Dirichlet: } \mathcal{B}_d(u)(\mathbf{z}) = u(\mathbf{z}),$$

$$(2.4) \quad \text{Neumann: } \mathcal{B}_n(u)(\mathbf{z}) = \rho(\mathbf{z}) \nabla u(\mathbf{z}) \cdot \mathbf{n}(\mathbf{z}),$$

$$(2.5) \quad \text{Periodic: } \mathcal{B}_\#(u)(\mathbf{z}) = u(\mathbf{z}) - u\left((z_i - n_i(\mathbf{z})L)_{i=1}^p, (z_i - n_i(\mathbf{z})\ell)_{i=p+1}^q\right).$$

The outer unit normal-vector is denoted by $\mathbf{n}(\mathbf{z})$ for $\mathbf{z} \in \partial\Omega_L$. In (2.2), we used the weighted Sobolev [49, 56] spaces as

$$(2.6) \quad H_{\mathcal{B}_x, \mathcal{B}_y}^1(\Omega_L; \rho) = \left\{ u \in H^1(\Omega_L; \rho) \mid \begin{cases} \mathcal{B}_x(u) = 0 & \text{on } \partial(0, L) \times (0, \ell) \\ \mathcal{B}_y(u) = 0 & \text{on } (0, L) \times \partial(0, \ell) \end{cases} \right\}$$

$$(2.7) \quad H^1(\Omega_L; \rho) = \left\{ u \in \mathcal{D}'(\Omega_L) \mid \|u\|_{H^1(\Omega_L; \rho)} < \infty \right\},$$

with $\mathcal{D}(\Omega_L) = C_c^\infty(\Omega_L)$ (the space of compactly supported test functions on Ω_L), which are equipped with the weighted norm

$$(2.8) \quad \|\cdot\|_{H^1(\Omega_L; \rho)} = \sqrt{\|\nabla \cdot\|_{L^2(\Omega_L; \rho)}^2 + \|\cdot\|_{L^2(\Omega_L; \rho)}^2},$$

for $\mathcal{B}_x, \mathcal{B}_y \in \{\mathcal{B}_d, \mathcal{B}_n, \mathcal{B}_\#\}$ and $\|\cdot\|_{L^2(\Omega_L; \rho)}^2 := \|\sqrt{\rho} \cdot\|_{L^2(\Omega_L)}^2$ in the classical L^2 -sense. The corresponding scalar product is $\langle \cdot, \cdot \rangle_{L^2(\Omega_L; \rho)} = \langle \rho \cdot, \cdot \rangle_{L^2(\Omega_L)}$.

Remark 2.2. If the weight ρ is zero only at the boundary of Ω_L , then we have $1/\rho \in L^1_{\text{loc}}(\Omega_L)$, which implies that $H^1_{\mathcal{B}_x, \mathcal{B}_y}(\Omega_L; \rho)$ is a Banach space [49, p235]. In the case of ρ being bounded from above and positive, i.e., $0 < \mathfrak{c} < \rho < \mathfrak{C}$ a.e. in Ω_L , the ρ -weighted Sobolev space from (2.6) is equivalent to the classical Sobolev space $H^1_{\mathcal{B}_x, \mathcal{B}_y}(\Omega_L; \rho) = H^1_{\mathcal{B}_x, \mathcal{B}_y}(\Omega_L)$, and we omit ρ in the notation.

Remark 2.3 (Weak form). The corresponding weak formulation of (2.2) reads: Find $(u, \lambda) \in (H^1_{\mathcal{B}_x, \mathcal{B}_y}(\Omega_L; \rho) \setminus \{0\}) \times \mathbb{R}$ such that

$$(2.9) \quad \forall v \in H^1_{\mathcal{B}_x, \mathcal{B}_y}(\Omega_L; \rho) : \quad \int_{\Omega_L} \rho \nabla u \cdot \nabla v \, dz + \int_{\Omega_L} V u v \, dz = \lambda \int_{\Omega_L} \rho u v \, dz.$$

Remark 2.4 (Min-max characterization). Since the weight ρ is a scalar function, (2.2) is self-adjoint for the presented boundary conditions, and we can express the eigenpair through the min-max characterization (c.f. [47, 36]):

$$(2.10) \quad \lambda^{(m)} = \min_{\substack{W_m \subset H^1_{\mathcal{B}_x, \mathcal{B}_y}(\Omega_L; \rho) \\ \dim W_m = m}} \max_{\substack{u \in W_m \\ u \neq 0}} \mathcal{R}_{\rho, V}(u),$$

with the Rayleigh quotient, defined by

$$(2.11) \quad \mathcal{R}_{\rho, V}(u) = \frac{\int_{\Omega_L} \rho(z) \nabla u(z) \cdot \nabla u(z) \, dz + \int_{\Omega_L} V(z) u^2(z) \, dz}{\int_{\Omega_L} \rho(z) u^2(z) \, dz},$$

which is identical for all the considered boundary conditions $\mathcal{B}_x, \mathcal{B}_y \in \{\mathcal{B}_d, \mathcal{B}_n, \mathcal{B}_\# \}$ of Definition 2.1.

We are now prepared to state our first main theoretical result:

THEOREM 2.5 (Factorization of eigenfunctions and summation of eigenvalues). *The m -th eigenfunction of the Schrödinger eigenvalue problem (1.2) can be factorized into*

$$(2.12) \quad u^{(m)}_{\mathcal{B}_d, \mathcal{B}_d, 1, V} = \psi \cdot u^{(m)} = \psi \cdot u_{x,1} \cdot u^{(m)}_{x,2} = \varphi_x \cdot u^{(m)}_{x,2}$$

$$(2.13) \quad = \psi \cdot u_{y,1} \cdot u^{(m)}_{y,2} = \varphi_y \cdot u^{(m)}_{y,2}$$

while the m -th eigenvalue can be summed correspondingly as

$$(2.14) \quad \lambda^{(m)}_{\mathcal{B}_d, \mathcal{B}_d, 1, V} = \lambda_\psi + \lambda^{(m)}_u = \lambda_\psi + \lambda_{u_{x,1}} + \lambda^{(m)}_{u_{x,2}} = \lambda_{\varphi_x} + \lambda^{(m)}_{u_{x,2}}$$

$$(2.15) \quad = \lambda_\psi + \lambda_{u_{y,1}} + \lambda^{(m)}_{u_{y,2}} = \lambda_{\varphi_y} + \lambda^{(m)}_{u_{y,2}}$$

where

$$(2.16) \quad \psi = u^{(1)}_{\mathcal{B}_\#, \mathcal{B}_\#, 1, V}, \quad u^{(m)} = u^{(m)}_{\mathcal{B}_d, \mathcal{B}_d, \psi^2, 0}, \quad u_{x,1} = u^{(1)}_{\mathcal{B}_d, \mathcal{B}_n, \psi^2, 0}, \quad u_{x,2} = u^{(m)}_{\mathcal{B}_n, \mathcal{B}_d, \varphi_x^2, 0},$$

$$(2.17) \quad u_{y,1} = u^{(1)}_{\mathcal{B}_n, \mathcal{B}_d, \psi^2, 0}, \quad u_{y,2} = u^{(m)}_{\mathcal{B}_d, \mathcal{B}_n, \varphi_y^2, 0}, \quad \varphi_x = u^{(1)}_{\mathcal{B}_d, \mathcal{B}_\#, 1, V}, \quad \varphi_y = u^{(1)}_{\mathcal{B}_\#, \mathcal{B}_d, 1, V}.$$

A graphical representation of Theorem 2.5 is presented in Figure 2 for $m = 1$, where the scale separation of, e.g., $\varphi_y^{(1)}$ into a short and $u_{y,2}^{(1)}$ into a large scale is visible. Moreover, the first excited eigenfunctions with $m \in \{2, 3, 4\}$ are visualized in Figure 3. Herein, we see that the m -dependence entirely goes into the $u_{y,2}^{(m)}$ function for the excited eigenfunctions since $\varphi_y^{(1)}$ is fixed.

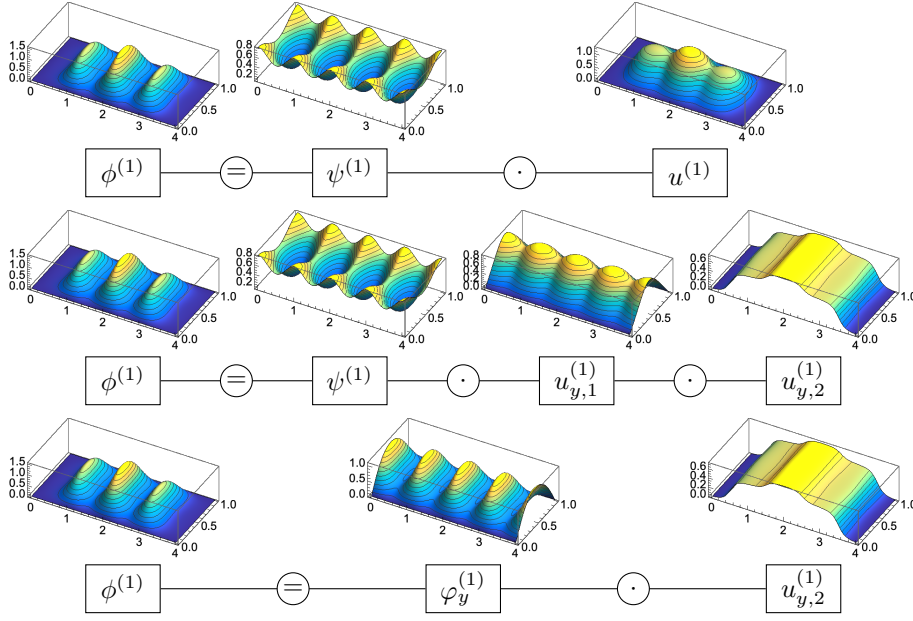


FIG. 2. Visualization of the factorization for the ground state solution of $-\Delta\phi^{(1)} + V\phi^{(1)} = \lambda^{(1)}\phi^{(1)}$, $\phi^{(1)} = 0$ on $\partial\Omega_4$ with $V(x, y) = 10^2(\sin x)^2(\sin y)^2$.

To prove [Theorem 2.5](#), we need to show that the factorizations are valid changes of variables. The application of the first *factorization principle* in [\(2.12\)](#), i.e.,

$$(2.18) \quad u_{\mathcal{B}_d, \mathcal{B}_d, \psi^2, 0}^{(m)} = u_{\mathcal{B}_d, \mathcal{B}_d, 1, V}^{(m)} / \psi,$$

removes the potential V from the eigenvalue problem while still encoding the corresponding information through ψ^2 . The inducing function $\psi = u_{\mathcal{B}_\#, \mathcal{B}_\#, 1, V}^{(1)}$ is the solution to a *spectral problem*, and it was shown in [\[6\]](#) that this factorization is indeed a diffeomorphism in $H_0^1(\Omega_L)$. Such factorization operators will apply a change of variables in the min-max characterization of the eigenvalue.

In contrast to [\(2.18\)](#) where ψ^2 is bounded from below a.e. by a positive constant, we will also need factorization operators induced by functions tending to zero at parts of the boundary due to homogeneous Dirichlet boundary conditions. In such cases, we need to adapt the factorization principle as the boundedness of the division operator is not directly visible, which makes the analysis much more subtle. Thus, we need:

LEMMA 2.6 (Factorization operator with degeneracy and singularity). *Let the inducing function $u_1 := u_{\mathcal{B}_n, \mathcal{B}_d, \psi^2, 0}^{(1)} \in H_{\mathcal{B}_n, \mathcal{B}_d}^1(\Omega_L)$ with $0 < c < \psi^2 < C$ a.e. be given. Then, the linear factorization operator defined by*

$$(2.19) \quad \begin{aligned} T : H_{\mathcal{B}_d, \mathcal{B}_d}^1(\Omega_L) &\rightarrow H_{\mathcal{B}_d, \mathcal{B}_n}^1(\Omega_L; u_1^2) \\ u &\mapsto T(u) := z \mapsto u(z)/u_1(z) \text{ a.e. in } \Omega_L \end{aligned}$$

is bi-continuous and thus a diffeomorphism.

Proof. Noting that T is a division operator, the corresponding multiplication operator T^{-1} is the (left and right) inverse operator. For a simpler notation, we use

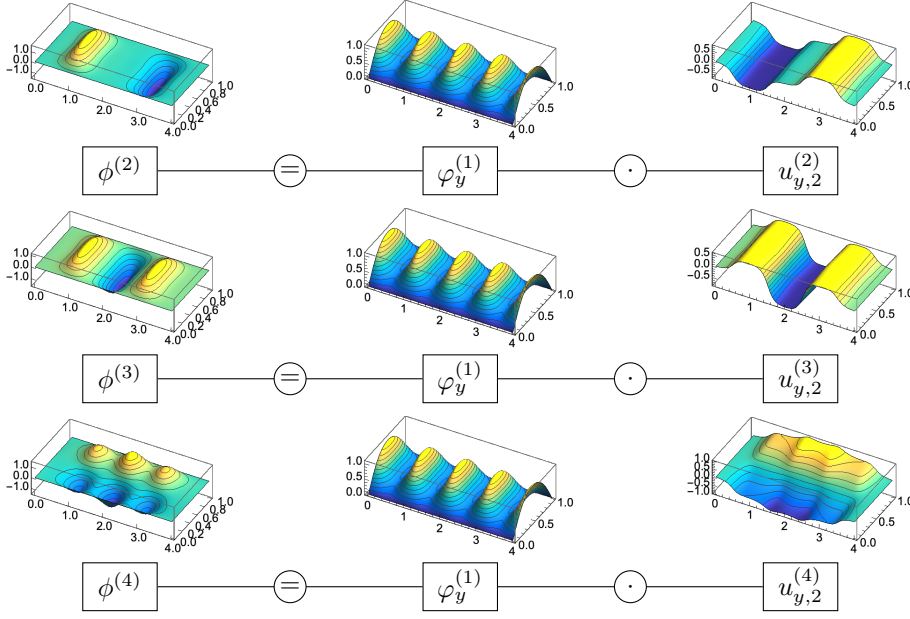


FIG. 3. Visualization of the factorization for some excited states of $-\Delta\phi^{(m)} + V\phi^{(m)} = \lambda^{(m)}\phi^{(m)}$ with $V(x, y) = 10^2(\sin x)^2(\sin y)^2$: By construction, the m -dependence entirely goes into the $u_{y,2}$ contribution.

$H_0^1(\Omega_L) = H_{\mathcal{B}_d, \mathcal{B}_d}^1(\Omega_L)$. So we study

$$(2.20) \quad \begin{aligned} \tilde{T} : H_0^1(\Omega_L) &\rightarrow W & \tilde{T}^{-1} : W &\rightarrow H_0^1(\Omega_L) \\ u &\mapsto u_2 := \tilde{T}(u) = \frac{u}{u_1} & u_2 &\mapsto u := \tilde{T}^{-1}(u_2) = u_1 u_2 \end{aligned}$$

with the abstract set $W := \text{Im}(\tilde{T}) = \text{Dom}(\tilde{T}^{-1})$ as

$$(2.21) \quad W = \left\{ u_2 \in \mathcal{D}'(\Omega_L) \mid \exists u \in H_0^1(\Omega_L) : u_2 = \tilde{T}(u) \right\}.$$

We first show that the image of \tilde{T} is the u_1^2 -induced weighted Sobolev space

$$(2.22) \quad H_{\mathcal{B}_d, \mathcal{B}_n}^1(\Omega_L; u_1^2) := \left\{ u_2 \in \mathcal{D}'(\Omega_L) \mid \tilde{T}^{-1}(u_2) \in H_0^1(\Omega_L), \begin{cases} \mathcal{B}_d(u_2) = 0 \text{ on } \partial\Omega_{\mathbf{x}} \times \Omega_{\mathbf{y}} \\ \mathcal{B}_n(u_2) = 0 \text{ on } \Omega_{\mathbf{x}} \times \partial\Omega_{\mathbf{y}} \end{cases} \right\}.$$

We have $W \subset \mathcal{D}'(\Omega_L)$ since $1/u_1 \in L_{\text{loc}}^1(\Omega_L)$ as $u_1 = 0$ only at the \mathbf{x} -boundary, and therefore $\forall \phi \in \mathcal{D}(\Omega_L) = C_c^\infty(\Omega_L)$, $\tilde{T}(\phi) = \int_{\Omega_L} \frac{1}{u_1} \phi < \|\phi\|_\infty \int_{\text{supp}(\phi)} \frac{1}{u_1} < \infty$ is a linear bounded functional since $\text{supp}(\phi)$ is compact. Then we have $W \subset H_{\mathcal{B}_d, \mathcal{B}_n}^1(\Omega_L; u_1^2)$ since $u_2 \in W$ implies that there exists a $u \in H_0^1(\Omega_L)$, such that $u_2 = \frac{u}{u_1}$, which yields $\mathcal{B}_d(u_2) = 0$ on $\partial\Omega_{\mathbf{x}}$ and trivially fulfilled $\mathcal{B}_n(u_2) = 0$ on $\partial\Omega_{\mathbf{y}}$, and allows us to take

$$(2.23) \quad \tilde{T}^{-1}(u_2) = u_1 u_2 = \frac{u_1}{u_1} u = u \in H_0^1(\Omega_L) \Rightarrow u_2 \in H_{\mathcal{B}_d, \mathcal{B}_n}^1(\Omega_L; u_1^2).$$

We also have $H_{\mathcal{B}_d, \mathcal{B}_n}^1(\Omega_L; u_1^2) \subset W$ since $u_2 \in H_{\mathcal{B}_d, \mathcal{B}_n}^1(\Omega_L; u_1^2)$ implies $\tilde{T}^{-1}(u_2) = u_1 u_2 = u \in H_0^1(\Omega_L)$ such that

$$(2.24) \quad \exists u \in H_0^1(\Omega_L) : u_2 = \frac{u}{u_1} = \tilde{T}(u) \Rightarrow u_2 \in W.$$

Thus $W = H_{\mathcal{B}_d, \mathcal{B}_n}^1(\Omega_L; u_1^2)$, so \tilde{T} defined by from (2.20) coincides with T from (2.19). Moreover, the weighted Sobolev space $H_{\mathcal{B}_d, \mathcal{B}_n}^1(\Omega_L; u_1^2)$ is a Banach space since u_1 only degenerates on the boundary (c.f. Remark 2.2).

Since T and T^{-1} are both surjective, T is bijective. We now show the continuity of T^{-1} as this is the more straightforward direction being a multiplication operator. Since all $u_{\mathcal{B}_d, \mathcal{B}_d, \psi^2, 0}^{(m)}$ form a basis of $H_0^1(\Omega_L)$ (c.f. subsection 2.1), it suffices to show continuity for all basis functions $u_{\mathcal{B}_d, \mathcal{B}_d, \psi^2, 0}^{(m)}$ and to conclude by linearity of the operator T^{-1} . Thus, let m be fixed, $u := u_{\mathcal{B}_d, \mathcal{B}_d, \psi^2, 0}^{(m)}$, and $u_2 := T(u_{\mathcal{B}_d, \mathcal{B}_d, \psi^2, 0}^{(m)})$. Then it follows for $u = T^{-1}(u_2) = u_1 u_2$ that

$$(2.25) \quad \int_{\Omega_L} \psi^2 \nabla u \cdot \nabla u dz = \int_{\Omega_L} \psi^2 u_1^2 \nabla u_2 \cdot \nabla u_2 dz + \int_{\Omega_L} \psi^2 \nabla u_1 \cdot \nabla (u_2^2 u_1) dz,$$

which is well defined by the assumption that u is the corresponding eigenfunction for the first expression in (2.25). We further have for the last term in (2.25) that

$$(2.26) \quad \int_{\Omega_L} \psi^2 \nabla u_1 \cdot \nabla (u_2^2 u_1) dz = - \int_{\Omega_L} \nabla \cdot (\psi^2 \nabla u_1) u_2^2 u_1 dz = \lambda_{u_1}^{(1)} \int_{\Omega_L} (\psi^2 u_1) (u_2^2 u_1) dz,$$

by the definition of $u_1 = u_{\mathcal{B}_n, \mathcal{B}_d, \psi^2, 0}^{(1)}$ according to (2.2) multiplied with $u_2^2 u_1$. Together with $0 < c < \psi^2 < C$, it then follows from (2.25) that

$$(2.27) \quad \begin{aligned} c \int_{\Omega_L} \nabla u \cdot \nabla u dz &\leq C \int_{\Omega_L} u_1^2 \nabla u_2 \cdot \nabla u_2 dz + C \lambda_{u_1}^{(1)} \int_{\Omega_L} u_1^2 u_2^2 dz \\ &\leq C \max \{1, \lambda_{u_1}^{(1)}\} \|u_2\|_{H^1(\Omega_L; u_1^2)}^2. \end{aligned}$$

Adding $\|u\|_{L^2(\Omega_L)}^2 = \|u_1 u_2\|_{L^2(\Omega_L)}^2 = \|u_2\|_{L^2(\Omega_L; u_1^2)}^2$ on both sides of (2.27) yields

$$(2.28) \quad \|\nabla u\|_{L^2(\Omega_L)}^2 + \|u\|_{L^2(\Omega_L)}^2 \leq \frac{C \max \{1, \lambda_{u_1}^{(1)}\}}{c} \|u_2\|_{H^1(\Omega_L; u_1^2)}^2 + \|u_2\|_{L^2(\Omega_L; u_1^2)}^2,$$

which finally, with $u_2 = T(u)$, provides us that $\|u\|_{H^1(\Omega_L)}^2 \leq D \|T(u)\|_{H^1(\Omega_L; u_1^2)}^2$ for some $D > 0$. This is equivalent to

$$(2.29) \quad \|T^{-1}(u_2)\|_{H^1(\Omega_L)}^2 \leq D \|u_2\|_{H^1(\Omega_L; u_1^2)}^2.$$

As T^{-1} is a linear, bijective, and continuous (by (2.29)) operator between two Banach spaces, the inverse $(T^{-1})^{-1} = T$ is also continuous [24, p35]. Thus $\|T(u)\|_{H^1(\Omega_L; u_1^2)}^2 \leq \tilde{D} \|u\|_{H^1(\Omega_L)}^2$. Bi-continuity of T implies that T and T^{-1} are continuously Fréchet-differentiable since they are both linear. Thus, T is a diffeomorphism [40]. \square

In order to apply the above-defined factorization operator in the min-max setting, we have the following:

LEMMA 2.7 (Rayleigh Quotients after Factorization). *Let $\phi = u_{\mathcal{B}_d, \mathcal{B}_d, 1, V}^{(m)}$, $u = u_{\mathcal{B}_d, \mathcal{B}_d, \psi^2, 0}^{(m)}$, and the first eigenpair $(\psi, \lambda_\psi) = (u, \lambda)_{\mathcal{B}_\#, \mathcal{B}_\#, 1, V}^{(1)}$ be given. Then, after the factorization $\phi = u \cdot \psi$, the corresponding Rayleigh quotient reads*

$$(2.30) \quad \mathcal{R}_{1, V}(\phi) = \mathcal{R}_{\psi^2, 0}(u) + \lambda_\psi.$$

Proof. We first note that the factorization allows for the splitting

$$(2.31) \quad \nabla \phi \cdot \nabla \phi = \nabla(u\psi) \cdot \nabla(u\psi) = \psi^2 \nabla u \cdot \nabla u + \nabla \psi \cdot \nabla(u^2 \psi).$$

A direct computation then shows that

$$(2.32) \quad \begin{aligned} \mathcal{R}_{1,V}(\phi) &= \frac{\int_{\Omega_L} \nabla(u\psi) \cdot \nabla(u\psi) dz + \int_{\Omega_L} V(u\psi)^2 dz}{\int_{\Omega_L} (u\psi)^2 dz} \\ &= \frac{\int_{\Omega_L} \psi^2 \nabla u \cdot \nabla u dz}{\int_{\Omega_L} \psi^2 u^2 dz} + \frac{\int_{\Omega_L} \nabla(u^2 \psi) \cdot \nabla \psi dz + \int_{\Omega_L} V(u^2 \psi) \psi dz}{\int_{\Omega_L} (u^2 \psi) \psi dz}. \end{aligned}$$

This calculation shows relation (2.30) since the second fraction is just the equation for ψ (see Definition 2.1) multiplied with $u^2 \psi$ as shown in, e.g., [10, p262] or [2, Lem. 2.1.]. \square

We can now combine all the above to prove Theorem 2.5:

Proof of Theorem 2.5. For a simpler notation, let

$$(2.33) \quad \phi = u_{\mathcal{B}_d, \mathcal{B}_{d,1}, V}^{(m)}, \quad \psi = u_{\mathcal{B}_\#, \mathcal{B}_\#, 1, V}^{(1)}, \quad u_1 = u_{\mathcal{B}_n, \mathcal{B}_d, \psi^2, 0}^{(1)}$$

by Definition 2.1. We apply the factorization principle twice with

$$(2.34) \quad \phi = u\psi = (T_\psi)^{-1}(u) \quad \text{and} \quad u = u_1 u_2 = (T_{u_1})^{-1}(u_2).$$

The operations are defined in (2.18) and Lemma 2.6, and the latter ensures that these are valid changes of variables in the min-max characterization. With Lemma 2.7 and the first change of variables, we then obtain for $\lambda_{\mathcal{B}_d, \mathcal{B}_{d,1}, V}^{(m)}$ that

$$(2.35) \quad \begin{aligned} \min_{\substack{W_m \subset H_{\mathcal{B}_d, \mathcal{B}_d}^1(\Omega_L) \\ \dim W_m = m}} \max_{\substack{\phi \in W_m \\ \phi \neq 0}} \mathcal{R}_{1,V}(\phi) &= \min_{\substack{W_m \subset H_{\mathcal{B}_d, \mathcal{B}_d}^1(\Omega_L) \\ \dim W_m = m}} \max_{\substack{u \in W_m \\ u \neq 0}} \mathcal{R}_{\psi^2, 0}(u) + \lambda_{\mathcal{B}_\#, \mathcal{B}_\#, 1, V}^{(1)} \\ &= \lambda_{\mathcal{B}_d, \mathcal{B}_d, \psi^2, 0}^{(m)} + \lambda_{\mathcal{B}_\#, \mathcal{B}_\#, 1, V}^{(1)}. \end{aligned}$$

The potential V is now encoded in the diffusion coefficient ψ^2 . We now continue in the same fashion with the second factorization and obtain

$$(2.36) \quad \begin{aligned} \lambda_{\mathcal{B}_d, \mathcal{B}_d, \psi^2, 0}^{(m)} &= \min_{\substack{W_m \subset H_{\mathcal{B}_d, \mathcal{B}_n}^1(\Omega_L; u_1^2) \\ \dim W_m = m}} \max_{\substack{u_2 \in W_m \\ u_2 \neq 0}} \mathcal{R}_{\psi^2 u_1^2, 0}(u_2) + \lambda_{\mathcal{B}_n, \mathcal{B}_d, \psi^2, 0}^{(1)} \\ &= \lambda_{\mathcal{B}_d, \mathcal{B}_n, \psi^2 u_1^2, 0}^{(m)} + \lambda_{\mathcal{B}_n, \mathcal{B}_d, \psi^2, 0}^{(1)}. \end{aligned}$$

Here, we used $(T_{u_1})^{-1}(u_2)$ being a diffeomorphism by Lemma 2.6 and, therefore, a well-defined change of variables, concluding the proof of (2.15). The corresponding eigenfunction multiplication in (2.13) is a direct result of the factorizations of (2.34). The other relations, i.e. (2.12) and (2.14), follow analogously with applying their respective factorizations $(T(\cdot))^{-1}$ in (2.34). \square

2.3. Homogenization in the Expanding Directions. In order to entirely characterize the asymptotic behavior of the spectrum as $L \rightarrow \infty$, we will now consider the contribution $\lambda_{\mathcal{B}_d, \mathcal{B}_n, \psi^2 u_1^2, 0}^{(m)}$ in (2.15) as the only one that depends on m after the factorization of Theorem 2.5. Then, we can make a precise statement about the asymptotic behavior of this remainder.

THEOREM 2.8 (Asymptotic behavior of expanding direction). *Let $\psi, u_{y,1}$ be given as in [Theorem 2.5](#) and define $\rho := (\psi u_{y,1})^2$. The asymptotic behavior of the eigenpair $(u, \lambda)_{\mathcal{B}_d, \mathcal{B}_n, \rho, 0}^{(m)}$ for $L \rightarrow \infty$ is*

$$(2.37) \quad \lambda_{\mathcal{B}_d, \mathcal{B}_n, \rho, 0}^{(m)} = \frac{1}{L^2} \left(\nu^{(m)} + o\left(\frac{1}{L}\right) \right),$$

$$(2.38) \quad L^{p/2} u_{\mathcal{B}_d, \mathcal{B}_n, \rho, 0}^{(m)}(\mathbf{x}/L, \mathbf{y}) \rightharpoonup u_0^{(m)}(\mathbf{x}) \text{ weakly up to a subseq. in } H_{\mathcal{B}_d, \mathcal{B}_n}^1(\Omega_1),$$

where $(u_0^{(m)}, \nu^{(m)}) \in (H_0^1((0,1)^p) \setminus \{0\}) \times \mathbb{R}$ is the solution to the p -dimensional homogenized eigenvalue problem

$$(2.39) \quad \begin{cases} -\nabla \cdot (\bar{D} \nabla u_0^{(m)}) = \nu^{(m)} \bar{C} u_0^{(m)} & \text{in } (0,1)^p \\ u_0^{(m)} = 0 & \text{on } \partial(0,1)^p \end{cases},$$

with the constant homogenized coefficients, $\bar{D} \in \mathbb{R}^{p \times p}$, $\bar{C} \in \mathbb{R}$, given by

$$(2.40) \quad \bar{D}_{ij} = \int_{(0,1)^p} \int_{(0,\ell)^q} \rho \left(\delta_{ij} + \frac{\partial \theta_j}{\partial x_i} \right) d\mathbf{y} d\mathbf{x}, \quad \bar{C} = \int_{(0,1)^p} \int_{(0,\ell)^q} \rho d\mathbf{y} d\mathbf{x},$$

for $i, j = 1, \dots, p$. The corrector functions $\{\theta_i(\mathbf{x}, \mathbf{y})\}_{1 \leq i \leq p}$ are defined as cell problem solutions on the periodic unit cell, as

$$(2.41) \quad \begin{cases} -\nabla \cdot (\rho(\tilde{\mathbf{x}}, \mathbf{y}) (\mathbf{e}_i + \nabla \theta_i(\tilde{\mathbf{x}}, \mathbf{y}))) = 0 & \text{in } \Omega_1 = (0,1)^p \times (0,\ell)^q \\ \tilde{\mathbf{x}} \mapsto \theta_i(\tilde{\mathbf{x}}, \mathbf{y}) & \tilde{\mathbf{x}}\text{-periodic} \end{cases}.$$

Furthermore, it holds that $\nu^{(1)} < \nu^{(2)}$.

Proof. To operate on fixed spatial domains, we map the problem from Ω_L to the reference domain $\Omega_1 = (0,1)^p \times (0,\ell)^q$ by $\mathbf{x} \mapsto \mathbf{x}/L =: \varepsilon \mathbf{x}$ and observe for the transformed weight function $\rho_\varepsilon(\mathbf{x}/\varepsilon, \mathbf{y})$ that $\rho_\varepsilon \in L_{\text{loc}}^1(\Omega_1)$ and $\rho_\varepsilon > 0$ a.e. in Ω_1 . Thus, the correct framework is the weighted space $H^1(\Omega_1; \rho_\varepsilon)$. We now encode the Dirichlet boundary conditions on the \mathbf{x} -boundary (as in [\[51, p6\]](#)) in the sense of traces with $\Gamma_D := \{0,1\}^p \times (0,\ell)^q \subset \partial\Omega_1$ in the subspace

$$(2.42) \quad \mathbb{V}_{\rho_\varepsilon} = \{\phi \in H^1(\Omega_1; \rho_\varepsilon) \mid \phi = 0 \text{ on } \Gamma_D\} \subset H^1(\Omega_1; \rho_\varepsilon).$$

Here, $\mathbb{V}_{\rho_\varepsilon} \subset H^1(\Omega_1; \rho_\varepsilon)$ is a Banach space since $\rho_\varepsilon = 0$ occurs only on the boundary Ω_1 (c.f. [Remark 2.2](#)). The weak form of the eigenvalue problem reads: Find $(u_\varepsilon^{(m)}, \lambda_\varepsilon^{(m)}) \in (\mathbb{V}_{\rho_\varepsilon} \setminus \{0\}) \times \mathbb{R}$, such that

$$(2.43) \quad \forall v \in \mathbb{V}_{\rho_\varepsilon} : \quad a_\varepsilon(u_\varepsilon^{(m)}, v) = \lambda_\varepsilon^{(m)} \int_{\Omega_1} \rho_\varepsilon(\mathbf{x}/\varepsilon, \mathbf{y}) u_\varepsilon^{(m)} v d\mathbf{x} d\mathbf{y},$$

with the bilinear form

$$(2.44) \quad a_\varepsilon(u_\varepsilon^{(m)}, v) = \int_{\Omega_1} \rho_\varepsilon(\mathbf{x}/\varepsilon, \mathbf{y}) \left(\frac{\partial u_\varepsilon^{(m)}}{\partial x_i} \frac{\partial v}{\partial x_i} + \frac{1}{\varepsilon^2} \frac{\partial u_\varepsilon^{(m)}}{\partial y_i} \frac{\partial v}{\partial y_i} \right) d\mathbf{x} d\mathbf{y},$$

using index notation. In [\(2.43\)](#), we moved the ε^2 -scaling to $\lambda_\varepsilon^{(m)}$ as

$$(2.45) \quad \lambda_{\mathcal{B}_d, \mathcal{B}_n, \rho_\varepsilon, 0}^{(m)} = \varepsilon^2 \lambda_\varepsilon^{(m)},$$

which follows from the min-max principle. This operation will be justified later when the existence of this ε^2 -transformed eigenvalue problem is shown for $\varepsilon \rightarrow 0$.

From [47, 48], we know that the homogenization of eigenvalue problems uses the same homogenized operators as for the corresponding source problem. Hence, we consider the bilinear form of the corresponding source problem to derive the homogenized operators. Therefore, given a family $f_\varepsilon(\mathbf{x}, \mathbf{y}) \in \mathbb{V}'_{\rho_\varepsilon}$ with $f_\varepsilon(\mathbf{x}, \mathbf{y}) \rightharpoonup f_0(\mathbf{x})$ in $\mathbb{V}'_{\rho_\varepsilon}$ weakly, we study the variational formulation

$$(2.46) \quad \forall v \in \mathbb{V}_{\rho_\varepsilon} : \quad a_\varepsilon(u_\varepsilon, v) = \langle f_\varepsilon, v \rangle_{\mathbb{V}'_{\rho_\varepsilon} \times \mathbb{V}_{\rho_\varepsilon}}.$$

The restriction of the family f_ε to \mathbf{y} -constant functions in the limit will be justified later when we show that the homogenized limit u_0 will have exactly this form. Thus, since we want to derive the eigenvalue problem from the source problem, f_ε has to mimic the properties of the sequence u_ε . The bilinear form $a_\varepsilon(u_\varepsilon, v)$ is $\mathbb{V}_{\rho_\varepsilon}$ -elliptic (for $\varepsilon \leq 1$), since $\forall u_\varepsilon \in \mathbb{V}_{\rho_\varepsilon}$, we have

$$(2.47) \quad \begin{aligned} a_\varepsilon(u_\varepsilon, u_\varepsilon) &\stackrel{\varepsilon \leq 1}{\geq} \|\nabla u_\varepsilon\|_{L^2(\Omega_1; \rho_\varepsilon)}^2 \stackrel{\text{F.-in.}}{\geq} \frac{1}{2} \|\nabla u_\varepsilon\|_{L^2(\Omega_1; \rho_\varepsilon)}^2 + \frac{C_F}{2} \|u_\varepsilon\|_{L^2(\Omega_1; \rho_\varepsilon)}^2 \\ &\geq \frac{1}{2} \min\{1, C_F\} \|u_\varepsilon\|_{H^1(\Omega_1; \rho_\varepsilon)}^2 =: C \|u_\varepsilon\|_{H^1(\Omega_1; \rho_\varepsilon)}^2, \end{aligned}$$

after using the weighted Friedrichs inequality [50, p199] (using the homogeneous Dirichlet boundary condition on parts of the boundary). Continuity also holds for all $\varepsilon > 0$ with a continuity constant proportional to $1/\varepsilon^2$. Thus, the problem is well-posed and admits a unique solution for all $\varepsilon > 0$ in $\mathbb{V}_{\rho_\varepsilon}$ (Lax–Milgram, c.f. [28, p126]). We, however, are interested in precisely the limit $\varepsilon \rightarrow 0$, which, at first, seems to be problematic since the continuity constant would tend to infinity if we do not further specify the $\partial \mathbf{y}$ -behavior in (2.44). However, we take (as in [51, p24]) u_ε in the bilinear form and use the coercivity to obtain

$$(2.48) \quad C \|u_\varepsilon\|_{H^1(\Omega_1; \rho_\varepsilon)}^2 \leq a_\varepsilon(u_\varepsilon, u_\varepsilon) = (f_\varepsilon, u_\varepsilon)_{L^2(\Omega_1; \rho_\varepsilon)} \leq \|f_\varepsilon\|_{H^{-1}(\Omega_1; \rho_\varepsilon)} \|u_\varepsilon\|_{H^1(\Omega_1; \rho_\varepsilon)}$$

with the operator norm $\|f_\varepsilon\|_{H^{-1}(\Omega_1; \rho_\varepsilon)} = \|f_\varepsilon\|_{\mathbb{V}'_{\rho_\varepsilon}} \rightarrow \|f_0\|_{\mathbb{V}'_{\rho_0}} \leq D$ by our assumption on the family $f_\varepsilon \in \mathbb{V}'_{\rho_\varepsilon}$. Therefore, u_ε is uniformly bounded in $H^1(\Omega_1; \rho_\varepsilon)$ since $\|u_\varepsilon\|_{H^1(\Omega_1; \rho_\varepsilon)} \leq \frac{1}{C} \|f_\varepsilon\|_{H^{-1}(\Omega_1; \rho_\varepsilon)} < \infty$. From the boundedness of u_ε in $H^1(\Omega_1; \rho_\varepsilon)$, we can follow with [59, Prop. 2.1.] that there exists a $u_0 \in H^1(\Omega_1; \rho_0(\mathbf{y}))$, such that there exists a converging subsequence of u_ε , still denoted by u_ε by abuse of notation, that weakly converges in $H^1(\Omega_1; \rho_0)$ where ρ_0 is the weak limit of ρ_ε . This ensures the existence of the desired homogenized limit u_0 of u_ε as $\varepsilon \rightarrow 0$. We can also directly infer $\sqrt{\rho_\varepsilon} \frac{\partial u_\varepsilon}{\partial \mathbf{y}} \rightarrow \mathbf{0}$ in $L^2(\Omega_1)$ by taking the limit in

$$(2.49) \quad \frac{C}{\varepsilon^2} \int_{\Omega_1} \rho_\varepsilon \left| \frac{\partial u_\varepsilon}{\partial \mathbf{y}} \right|^2 \leq a_\varepsilon(u_\varepsilon, u_\varepsilon) \leq \|f_\varepsilon\|_{H^{-1}(\Omega_1; \rho_\varepsilon)} \|u_\varepsilon\|_{H^1(\Omega_1; \rho_\varepsilon)} \leq \frac{1}{C} \|f_\varepsilon\|_{H^{-1}(\Omega_1; \rho_\varepsilon)}^2 < \infty,$$

since the norm of u_ε is bounded by the norm of f_ε , which implies that

$$(2.50) \quad \lim_{\varepsilon \rightarrow 0} \left\| \sqrt{\rho_\varepsilon} \frac{\partial u_\varepsilon}{\partial \mathbf{y}} - \mathbf{0} \right\|_{L^2(\Omega_1)} = 0,$$

since $\frac{1}{C} \|f_\varepsilon\|_{H^{-1}(\Omega_1; \rho_\varepsilon)}^2$ is bounded for all ε including $\varepsilon = 0$. Therefore $\sqrt{\rho_\varepsilon} \frac{\partial u_\varepsilon}{\partial \mathbf{y}} \rightarrow \mathbf{0}$ in $L^2(\Omega_1)$, which will be important later to reduce the dimension of the homogenized

equation from $p + q$ dimensions to just p . Since ρ_0 is nonzero a.e. on Ω_1 (recall that $\rho_\varepsilon = 0$ only happens on the \mathbf{y} -boundary), we have $\frac{\partial u_\varepsilon}{\partial \mathbf{y}} \rightarrow \mathbf{0}$ in $L^2(\Omega_1)$. Thus, a homogenized limit u_0 with $\partial u_0 / \partial \mathbf{y} = \mathbf{0}$ exists for the sequence u_ε .

Since we know that there exists a homogenized limit u_0 , we aim to derive the corresponding homogenized equation for u_0 . Therefore, consider

$$(2.51) \quad \xi_\varepsilon(\mathbf{x}, \mathbf{y}) := \sqrt{\rho_\varepsilon(\mathbf{x}/\varepsilon, \mathbf{y})} \nabla u_\varepsilon(\mathbf{x}, \mathbf{y}).$$

Following the usual arguments [51, p24], from the uniform boundedness of u_ε , it follows that

$$(2.52) \quad \|\xi_\varepsilon\|_{L^2(\Omega_1)} = \|u_\varepsilon\|_{H^1(\Omega_1; \rho_\varepsilon)} \leq \|u_\varepsilon\|_{H^1(\Omega_1; \rho_\varepsilon)} \leq \frac{1}{C} \|f\|_{H^{-1}(\Omega_1; \rho_\varepsilon)} < \infty.$$

Therefore, we can again extract subsequences ξ_ε , still denoted by ξ_ε , such that $\xi_\varepsilon \rightharpoonup \xi_0$ in $L^2(\Omega_1)$ weakly. This convergence implies that the equation of interest

$$(2.53) \quad \langle \xi_\varepsilon, \nabla v \rangle_{L^2(\Omega_1)} = \langle f_\varepsilon, v \rangle_{\mathbb{V}_{\rho_\varepsilon}} \quad \forall v \in \mathbb{V}_{\rho_\varepsilon},$$

has a limit for $\varepsilon \rightarrow 0$ as

$$(2.54) \quad \langle \xi_0, \nabla v \rangle_{L^2(\Omega_1)} = \langle f_0, v \rangle_{\mathbb{V}_{\rho_0}} \quad \forall v \in \mathbb{V}_{\rho_0}.$$

To explicitly state this limit equation, we need to calculate ξ_0 . We employ the oscillatory test function method [4, p10] to overcome the problem of $\xi_\varepsilon = \sqrt{\rho(\mathbf{x}/\varepsilon, \mathbf{y})} \nabla u_\varepsilon$ being a product of two weakly converging functions and thus not simply being the product of both limits for $\varepsilon \rightarrow 0$. We need to adapt the method to account for the directional periodicity and the additional ε^{-2} -scaling of the $(\partial u_\varepsilon / \partial y_i)$ -term in the bilinear form (2.44). Thus, let $\varphi \in \mathcal{D}((0, 1)^p)$ be a smooth, only \mathbf{x} -dependent, and compactly supported test function (i.e., $\varphi \in C_c^\infty((0, 1)^p)$). Then, inspired by the first two terms in the asymptotic expansion for u_ε , we define the test function φ_ε as

$$(2.55) \quad \varphi_\varepsilon(\mathbf{x}, \mathbf{y}) := \varphi(\mathbf{x}) + \varepsilon \sum_{i=1}^p \frac{\partial \varphi}{\partial x_i}(\mathbf{x}) \theta_i(\mathbf{x}/\varepsilon, \mathbf{y})$$

where, with $\tilde{\mathbf{x}} := \mathbf{x}/\varepsilon$, $\theta_i(\tilde{\mathbf{x}}, \mathbf{y})$ is the solution the corrector problem (2.41), which admits for all $i = 1, \dots, p$ a unique (up to a constant) solution $\theta_i \in (H^1(\Omega_1; \rho_1) \setminus \mathbb{R})$ (due to periodic boundary conditions). Since $\theta_i(\tilde{\mathbf{x}}, \mathbf{y})$ is $\tilde{\mathbf{x}}$ -periodic, it converges weakly to its average in $H^1(\Omega_1; \rho_\varepsilon)$ as $\varepsilon \rightarrow 0$. Thus, the expression $\varepsilon \theta_i(\tilde{\mathbf{x}}, \mathbf{y})$ in (2.55) converges to zero since $\varepsilon \rightarrow 0$. This implies that φ_ε has a well-defined limit $\varphi_\varepsilon \rightharpoonup \varphi_0 = \varphi(\mathbf{x})$ for $\varepsilon \rightarrow 0$.

In the following, we make use of the notations

$$(2.56) \quad \nabla(\cdot) := \begin{pmatrix} \nabla_{\mathbf{x}}(\cdot) \\ \nabla_{\mathbf{y}}(\cdot) \end{pmatrix}, \quad D_{\mathbf{x}/\tilde{\mathbf{x}}}(\cdot) := \begin{pmatrix} \nabla_{\mathbf{x}/\tilde{\mathbf{x}}}(\cdot) \\ 0 \end{pmatrix}, \quad D_{\mathbf{y}}(\cdot) := \begin{pmatrix} 0 \\ \nabla_{\mathbf{y}}(\cdot) \end{pmatrix},$$

with the grouping of into (p, q) -blocks. As the derivative of φ_ε is required in the variational formulation, we derive from (2.55), using the chain and product rule, that

$$(2.57) \quad \nabla \varphi_\varepsilon = \sum_{i=1}^p \frac{\partial \varphi}{\partial x_i} (e_i + D_{\tilde{\mathbf{x}}} \theta_i(\tilde{\mathbf{x}}, \mathbf{y}) + \varepsilon D_{\mathbf{y}} \theta_i(\tilde{\mathbf{x}}, \mathbf{y})) + \varepsilon \sum_{i=1}^p \left(\frac{\partial (D_{\mathbf{x}} \varphi)}{\partial x_i}(\mathbf{x}) \theta_i(\tilde{\mathbf{x}}, \mathbf{y}) \right).$$

We then insert the test function φ_ε into the bilinear form (2.44) to obtain (2.58)

$$\begin{aligned} a_\varepsilon(u_\varepsilon, \varphi_\varepsilon) &= \int_{\Omega_1} \rho_\varepsilon(\tilde{\mathbf{x}}, \mathbf{y}) \nabla u_\varepsilon \cdot \left(\sum_{i=1}^p \frac{\partial \varphi}{\partial x_i} (e_i + D_{\tilde{\mathbf{x}}} \theta_i(\tilde{\mathbf{x}}, \mathbf{y}) + \varepsilon^{-1} D_{\mathbf{y}} \theta_i(\tilde{\mathbf{x}}, \mathbf{y})) \right) \\ &\quad + \varepsilon \int_{\Omega_1} \rho_\varepsilon(\tilde{\mathbf{x}}, \mathbf{y}) \nabla u_\varepsilon \cdot \left(\sum_{i=1}^p \left(\frac{\partial(D_{\mathbf{x}} \varphi)}{\partial x_i}(\mathbf{x}) \theta_i(\tilde{\mathbf{x}}, \mathbf{y}) \right) \right). \end{aligned}$$

The last term in (2.58) can be bounded by a constant times ε by the Cauchy–Schwarz inequality since the (φ, θ_i) -term is in $L^2(\Omega_1; \rho_\varepsilon)$ and $\nabla u_\varepsilon \in L^2(\Omega_1; \rho_\varepsilon)$ and thus vanishes in the limit. Integration by parts (with Dirichlet in \mathbf{x} - and trivially fulfilled Neumann data in \mathbf{y} -direction) in the other term of (2.58) yields

$$\begin{aligned} (2.59) \quad & \int_{\Omega_1} \rho_\varepsilon(\tilde{\mathbf{x}}, \mathbf{y}) \nabla u_\varepsilon \cdot \left(\sum_{i=1}^p \frac{\partial \varphi}{\partial x_i}(\mathbf{x}) (e_i + D_{\tilde{\mathbf{x}}} \theta_i(\tilde{\mathbf{x}}, \mathbf{y}) + \varepsilon^{-1} D_{\mathbf{y}} \theta_i(\tilde{\mathbf{x}}, \mathbf{y})) \right) \\ &= - \int_{\Omega_1} u_\varepsilon \nabla \cdot \left(\rho_\varepsilon(\tilde{\mathbf{x}}, \mathbf{y}) \sum_{i=1}^p \frac{\partial \varphi}{\partial x_i}(\mathbf{x}) (e_i + D_{\tilde{\mathbf{x}}} \theta_i(\tilde{\mathbf{x}}, \mathbf{y}) + \varepsilon^{-1} D_{\mathbf{y}} \theta_i(\tilde{\mathbf{x}}, \mathbf{y})) \right). \end{aligned}$$

The divergence term in (2.59) can be further simplified to (2.60)

$$\begin{aligned} & \nabla \cdot \left(\rho_\varepsilon(\tilde{\mathbf{x}}, \mathbf{y}) \sum_{i=1}^p \frac{\partial \varphi}{\partial x_i}(\mathbf{x}) (e_i + D_{\tilde{\mathbf{x}}} \theta_i(\tilde{\mathbf{x}}, \mathbf{y}) + \varepsilon^{-1} D_{\mathbf{y}} \theta_i(\tilde{\mathbf{x}}, \mathbf{y})) \right) \\ &= \sum_{i=1}^p \frac{\partial(D_{\mathbf{x}} \varphi)}{\partial x_i}(\mathbf{x}) \cdot \rho_\varepsilon(\tilde{\mathbf{x}}, \mathbf{y}) (e_i + D_{\tilde{\mathbf{x}}} \theta_i(\tilde{\mathbf{x}}, \mathbf{y})) \\ &\quad + \varepsilon^{-1} \sum_{i=1}^p \frac{\partial \varphi}{\partial x_i}(\mathbf{x}) [D_{\tilde{\mathbf{x}}} \cdot (\rho_\varepsilon(\tilde{\mathbf{x}}, \mathbf{y}) (e_i + D_{\tilde{\mathbf{x}}} \theta_i(\tilde{\mathbf{x}}, \mathbf{y}))) + D_{\mathbf{y}} \cdot (\rho_\varepsilon(\tilde{\mathbf{x}}, \mathbf{y}) D_{\mathbf{y}} \theta_i(\tilde{\mathbf{x}}, \mathbf{y}))]. \end{aligned}$$

We can combine the two last terms of (2.60) to extract

$$(2.61) \quad \varepsilon^{-1} \left(\frac{\nabla \tilde{\mathbf{x}}}{\nabla \mathbf{y}} \right) \cdot \left(\rho_\varepsilon(\tilde{\mathbf{x}}, \mathbf{y}) \left(e_i + \left(\frac{\nabla \tilde{\mathbf{x}}}{\nabla \mathbf{y}} \right) \theta_i(\tilde{\mathbf{x}}, \mathbf{y}) \right) \right),$$

which is zero (even for $\varepsilon \rightarrow 0$) due to the particular definition of the corrector θ_i in (2.41). Here, we notice that the ε^{-2} -scaling in the \mathbf{y} -term of the initial expression precisely aligns with the extruding additional ε^{-1} that appeared in (2.61) by the chain rule. Thus, the only remaining term of (2.60) is

$$(2.62) \quad \sum_{i=1}^p \frac{\partial(D_{\mathbf{x}} \varphi)}{\partial x_i}(\mathbf{x}) \cdot \rho_\varepsilon(\tilde{\mathbf{x}}, \mathbf{y}) (e_i + D_{\tilde{\mathbf{x}}} \theta_i(\tilde{\mathbf{x}}, \mathbf{y})),$$

bounded in $L^2(\Omega_1)$ and, thus, weakly converges as $\varepsilon \rightarrow 0$ to its average in $\tilde{\mathbf{x}}$ -direction [4, Lem. 1.8.].

In (2.59), now recall that u_ε converges strongly to u_0 in $L^2(\Omega_1; \rho_0)$ (by the Rellich theorem, c.f. [3, 4.3.21]). Thus, we can take the limit of the right-hand side in (2.59). So in total, we can take the limit of (2.58), which is the product of the limit of $u_\varepsilon \rightarrow u_0$ (strongly) with the weak limit (2.62) of the divergence term. Thus the weak

form (2.46) reduces in the $(\varepsilon \rightarrow 0)$ -limit to

$$\begin{aligned}
 & - \int_{\Omega_1} u_0(\mathbf{x}) \nabla \cdot \left(\int_{(0,1)^p} \rho_0(\tilde{\mathbf{x}}, \mathbf{y}) \sum_{i=1}^p \frac{\partial \varphi}{\partial x_i}(\mathbf{x}) (e_i + D_{\tilde{\mathbf{x}}} \theta_i(\tilde{\mathbf{x}}, \mathbf{y})) d\tilde{\mathbf{x}} \right) d\mathbf{x} d\mathbf{y} \\
 (2.63) \quad & = \lim_{\varepsilon \rightarrow 0} \int_{\Omega_1} \rho_\varepsilon(\tilde{\mathbf{x}}, \mathbf{y}) \nabla u_\varepsilon(\mathbf{x}, \mathbf{y}) \cdot \nabla \varphi_\varepsilon(\mathbf{x}, \mathbf{y}) = \lim_{\varepsilon \rightarrow 0} \int_{\Omega_1} \rho_\varepsilon(\tilde{\mathbf{x}}, \mathbf{y}) f_\varepsilon(\mathbf{x}, \mathbf{y}) \varphi_\varepsilon(\mathbf{x}, \mathbf{y}) \\
 & = \int_{\Omega_1} \rho_0(\mathbf{y}) f_0(\mathbf{x}) \varphi(\mathbf{x}).
 \end{aligned}$$

We can rewrite the left-hand side of (2.63) using a compact notation as

$$\begin{aligned}
 (2.64) \quad & \left[\int_{(0,1)^p} \rho_1(\tilde{\mathbf{x}}, \mathbf{y}) \sum_{i=1}^p \frac{\partial \varphi}{\partial x_i}(\mathbf{x}) (e_i + D_{\tilde{\mathbf{x}}} \theta_i(\tilde{\mathbf{x}}, \mathbf{y})) d\tilde{\mathbf{x}} \right]_j \\
 & = \sum_{i=1}^p \frac{\partial \varphi}{\partial x_i}(\mathbf{x}) \int_{(0,1)^p} \rho_1(\tilde{\mathbf{x}}, \mathbf{y}) \left(\delta_{ij} + \frac{\partial \theta_i}{\partial \tilde{x}_j} \right) d\tilde{\mathbf{x}} =: \sum_{i=1}^p \frac{\partial \varphi}{\partial x_i}(\mathbf{x}) \tilde{D}_{ji}(\mathbf{y}),
 \end{aligned}$$

where we identify the last expression as $[\tilde{D}^T(\mathbf{y}) \nabla \varphi(\mathbf{x})]_j$. As the last step, we reverse the integration by parts and obtain the variational formulation of the homogenized equation for u_0 , which is still posed on the $(p+q)$ -dimensional domain Ω_1 , but with u_0 only \mathbf{x} -dependent according to (2.50). The problem then reads: Find $u_0(\mathbf{x}) \in \mathbb{V}_{\rho_0}$, such that

$$(2.65) \quad \int_{\Omega_1} \tilde{D}(\mathbf{y}) \nabla u_0(\mathbf{x}) \cdot \nabla \varphi(\mathbf{x}) d\mathbf{x} d\mathbf{y} = \int_{\Omega_1} \tilde{C}(\mathbf{y}) f_0(\mathbf{x}) \varphi(\mathbf{x}) d\mathbf{x} d\mathbf{y} \quad \forall \varphi \in C_c^\infty((0,1)^p),$$

with the \mathbf{y} -dependent operators

$$(2.66) \quad \tilde{D}_{ij}(\mathbf{y}) = \int_{(0,1)^p} \rho_1(\tilde{\mathbf{x}}, \mathbf{y}) \left(\delta_{ij} + \frac{\partial \theta_j}{\partial \tilde{x}_i} \right) d\tilde{\mathbf{x}}, \quad \tilde{C}(\mathbf{y}) = \int_{(0,1)^p} \rho_1(\tilde{\mathbf{x}}, \mathbf{y}) d\tilde{\mathbf{x}},$$

for $i, j = 1, \dots, p$. In (2.66), we remark that these operators look very similar to the usual homogenized operators, e.g., in [6], with the difference that the integration only takes place in the p expanding directions over $(0,1)^p$.

In our setup, we can, however, further reduce the homogenized limit equation (2.65) since, by definition, $\nabla \varphi(\mathbf{x}) = D_{\mathbf{x}} \varphi(\mathbf{x})$. This allows us to concretize further that $u_0(\mathbf{x}) \in H_0^1((0,1)^p)$ since $u_0(\mathbf{x}) \in \mathbb{V}_{\rho_0(\mathbf{y})}$ implies $u_0(\mathbf{x}) = 0$ on $\partial(0,1)^p$ and $\|u_0(\mathbf{x})\|_{H^1((0,1)^p)} < \infty$ since for any $u(\mathbf{x}) \in H^1(\Omega_1; \rho_0)$ with $\rho_0(\mathbf{y}) > 0$ a.e. in $(0, \ell)^q$, it holds that

$$(2.67) \quad \|u(\mathbf{x})\|_{H^1(\Omega_1; \rho_0)}^2 = \left(\int_{(0,1)^q} \rho_0(\mathbf{y}) d\mathbf{y} \right) \|u(\mathbf{x})\|_{H^1((0,1)^p)}^2 = \overline{\rho_0}^y \|u(\mathbf{x})\|_{H^1((0,1)^p)}^2 < \infty,$$

since $\overline{\rho_0}^y \in \mathbb{R}$ is a strictly positive constant. Thus, the homogenized equation reduces from the $(p+q)$ - to the p -dimensional variational problem: Find $u_0 \in H_0^1((0,1)^p)$, such that

$$(2.68) \quad \int_{(0,1)^p} \bar{D} \nabla u_0(\mathbf{x}) \cdot \nabla \varphi(\mathbf{x}) d\mathbf{x} = \int_{(0,1)^p} \bar{C} f_0(\mathbf{x}) \varphi(\mathbf{x}) d\mathbf{x} \quad \forall \varphi \in C_c^\infty((0,1)^p),$$

with the constant homogenized coefficients, defined by (2.40), as the integral of $\tilde{C}(\mathbf{y})$ and $\tilde{D}(\mathbf{y})$ from (2.66) over $(0, 1)^q$.

The homogenized equation (2.68) is formulated on $H_0^1((0, 1)^p)$. Recall that $\varphi \in C_c^\infty((0, 1)^p)$ was chosen arbitrarily. Since $C_c^\infty((0, 1)^p)$ is dense in $H_0^1((0, 1)^p)$ by the definition of H_0^1 as the closure of C_c^∞ under the H^1 -norm [3, Def. 4.3.8.], (2.65) holds $\forall \varphi \in H_0^1((0, 1)^p)$. As the homogenized operator satisfies coercivity (c.f. [51, Rem. 2.6.]), the theorem of Lax–Milgram ensures the uniqueness of the homogenized limit u_0 . This, on the other hand, implies that any subsequence of u_ε converges to u_0 in the limit. Thus, the entire sequence u_ε converges to the same limit u_0 following the standard arguments from, e.g., [4].

Since we now have derived the homogenized equation for the source problem, we can directly deduce from [47, Thm. 2.1.] that the eigenvalues and -functions converge to the homogenized eigenvalue equation, posed with the same operator as in (2.68), resulting in

$$(2.69) \quad (\lambda_\varepsilon^{(m)}, u_\varepsilon^{(m)}) \rightarrow (\nu^{(m)}, u_0^{(m)}) \text{ in } \mathbb{R} \times (H_0^1((0, 1)^p) \text{ weakly up to subseq.}),$$

where the homogenized eigenpair is defined through (2.39). The convergence of the eigenfunctions holds up to a subsequence because of the eigenvalue multiplicity of the homogenized limit. To account for the normalization constraint after the initial transformation $\mathbf{x} \mapsto \varepsilon \mathbf{x}$, we note that $\|u_0(\cdot, \cdot)\|_{L^2(\Omega_L)} = L^{p/2} \|u_0(\cdot/L, \cdot)\|_{L^2(\Omega_1)}$ by the transformation rule and recall the $(1/L^2)$ -scaling from (2.45) for the eigenvalues, which implies (2.37).

The limit eigenvalue $\nu^{(m)}$ is simple and $\nu^{(1)} < \nu^{(2)} < \nu^{(3)} < \dots \rightarrow \infty$ by the Sturm–Liouville theory for the particular case of $p = 1$ with $\bar{D}_{11}, \bar{C} > 0$. Furthermore, we have $\nu^{(1)} < \nu^{(2)} \leq \nu^{(3)} \leq \dots \rightarrow \infty$ for the general case of $p \geq 2$ since the eigenvalue problem is elliptic, but multiplicities could exceed one for higher eigenvalues. \square

We are now ready to prove the optimality of the spectral shift $\sigma = \lambda_{\varphi_y}$:

THEOREM 2.9. *For the optimal shift $\sigma = \lambda_{\varphi_y} = \lambda_{\mathcal{B}_\#, \mathcal{B}_d, 1, V}^{(1)}$, the asymptotic shifted fundamental eigenvalue ratio of the linear periodic Schrödinger eigenvalue problem (1.2) converges to a positive constant $C < 1$ as $L \rightarrow \infty$, that is*

$$(2.70) \quad 0 \leq \frac{\lambda_{\mathcal{B}_d, \mathcal{B}_d, 1, V}^{(1)} - \lambda_{\mathcal{B}_\#, \mathcal{B}_d, 1, V}^{(1)}}{\lambda_{\mathcal{B}_d, \mathcal{B}_d, 1, V}^{(2)} - \lambda_{\mathcal{B}_\#, \mathcal{B}_d, 1, V}^{(1)}} = \frac{\lambda_{\mathcal{B}_d, \mathcal{B}_n, \varphi_y^2, 0}^{(1)}}{\lambda_{\mathcal{B}_d, \mathcal{B}_n, \varphi_y^2, 0}^{(2)}} \rightarrow C < 1.$$

Proof. The proof follows from Theorem 2.8 since $L^2 \lambda_{\mathcal{B}_d, \mathcal{B}_n, \varphi_y^2, 0}^{(m)} = \nu^{(m)} + o(\frac{1}{L})$ and $\nu^{(1)} < \nu^{(2)}$. \square

We will see later that pre-asymptotic effects lead to a non-monotonic convergence of (2.70). However, since the convergence holds in the limit, we can make a statement for uniform boundedness if L is sufficiently large.

COROLLARY 2.10. *There exists a constant $D \in [0, 1)$ and a length $L^* \in \mathbb{R}^+$, such that the optimally shifted ratio from Theorem 2.9 is uniformly bounded from above by D for all $L > L^*$. That is*

$$(2.71) \quad \exists D \in [0, 1) \exists L^* \in \mathbb{R}^+ : 0 \leq \frac{\lambda_{\mathcal{B}_d, \mathcal{B}_d, 1, V}^{(1)} - \lambda_{\mathcal{B}_\#, \mathcal{B}_d, 1, V}^{(1)}}{\lambda_{\mathcal{B}_d, \mathcal{B}_d, 1, V}^{(2)} - \lambda_{\mathcal{B}_\#, \mathcal{B}_d, 1, V}^{(1)}} < D < 1 \quad \forall L > L^*.$$

Proof. The proof follows directly from the convergence result of Theorem 2.9. \square

[Theorem 2.8](#) gives an abstract description of the homogenized equation. However, for our present setup, we can even solve the equation analytically (which will be important later in [subsection 4.1](#)):

Remark 2.11. The homogenization problem in [Theorem 2.8](#) is posed with an isotropic operator ρI , and ρ is either periodic or zero on the boundaries. Thus every column of ρI is a solenoidal vector field in the integral sense by the divergence theorem. Hence, we can conclude with [\[46, p17\]](#) that the homogenized operator is diagonal. Then, the diagonality allows us to explicitly state the homogenized eigenpairs as the Laplacian eigenfunctions on the hyper rectangle with scaled Laplacian eigenvalues as $\nu^{(m)} = \pi^2 (\sum_{i=1}^p \bar{D}_{ii} m_i^2) / \bar{C}$ and $u^{(m)}(\mathbf{x}) = \mathcal{N}^{(m)} \prod_i^p \sin(m_i \pi x_i)$, where the set $\mathcal{M} = \{m_i, \dots, m_p\} \in \mathbb{N}^p, |\mathcal{M}| = m$, is chosen to minimize $\nu^{(m)}$. The factors $\mathcal{N}^{(m)}$ are defined by the normalization condition $\int_{(0,1)^p} \bar{C} (u^{(m)})^2 = 1$.

We now return to the convergence properties of the eigenvalue solvers. [Theorem 2.9](#) implies a constant number of iterations for all eigensolvers that are shift-and-invert preconditioned with $\sigma = \lambda_{\mathcal{B}_{\#}, \mathcal{B}_d, 1, V}^{(1)}$ and depend on the fundamental ratio. Using this strategy, the eigensolver can reach a given residual norm with a constant number of iterations for all $L \rightarrow \infty$.

3. Spatial Discretization and Iterative Eigensolvers. To solve the eigenvalue problem [\(1.2\)](#) numerically, we will discretize the continuous equation on a finite-dimensional space. Then, we solve the resulting system with a preconditioned algebraic eigensolver.

3.1. Galerkin Finite Element Approach. Consider a conforming and shape-regular partition \mathcal{T}_h of the domain Ω_L into finite elements $\tau \in \mathcal{T}_h$, which have a polygonal shape. We write \mathcal{T}_h for partitions where every element has a diameter of at most $2h$ [\[52, p36\]](#). Define the finite element subspace $\mathbb{H}_h(\Omega_L) \subset H_0^1(\Omega_L)$, consisting of polynomial functions with total degree r from the polynomial space \mathcal{P}_r , to be $\mathbb{H}_h(\Omega_L) = \{u \in H_0^1(\Omega_L) \mid u|_{\tau} \in \mathcal{P}_r(\tau) \forall \tau \in \mathcal{T}_h\}$. We then search for a discrete solution $\phi_h^{(m)} \in (\mathbb{H}_h(\Omega_L) \setminus \{0\})$, such that

$$(3.1) \quad \forall v_h \in \mathbb{H}_h(\Omega_L) : \quad \int_{\Omega_L} A \nabla \phi_h^{(m)} \cdot \nabla v_h d\mathbf{z} + \int_{\Omega_L} V \phi_h^{(m)} v_h d\mathbf{z} = \lambda_h^{(m)} \int_{\Omega_L} \phi_h^{(m)} v_h d\mathbf{z}.$$

For the coefficient vector \mathbf{x}_h of a given basis, we obtain the equivalent generalized algebraic eigenvalue problem: Find $\mathbf{x}_h^{(m)} \in \mathbb{R}^n \setminus \{\mathbf{0}\}$, such that

$$(3.2) \quad \mathbf{A} \mathbf{x}_h^{(m)} = \lambda_h^{(m)} \mathbf{B} \mathbf{x}_h^{(m)},$$

where $\mathbf{A} \in \mathbb{R}^{n \times n}$ consists of the usual stiffness matrix plus the contribution from the potential and $\mathbf{B} \in \mathbb{R}^{n \times n}$ denotes the mass matrix. Both \mathbf{A} and \mathbf{B} as finite representations of the continuous operators in [\(1.2\)](#) are symmetric positive definite. Since the discrete problem is formulated on a subspace $\mathbb{H}_h(\Omega_L) \subset H_0^1(\Omega_L)$, we have by the min-max characterization that $\lambda^{(m)} \leq \lambda_h^{(m)}$. Furthermore, we have $\lambda_h^{(m)} \rightarrow \lambda^{(m)}$ for $h \rightarrow 0$ [\[20, 52\]](#).

For the calculation of the optimal shift λ_{φ_y} , we solve

$$(3.3) \quad \forall v_h \in \mathbb{H}_h^{\varphi_y}(\Omega_1) : \quad \int_{\Omega_1} A \nabla \varphi_{y,h}^{(1)} \cdot \nabla v_h d\mathbf{z} + \int_{\Omega_1} V \varphi_{y,h}^{(1)} v_h d\mathbf{z} = \lambda_{\varphi_y,h}^{(1)} \int_{\Omega_L} \varphi_{y,h}^{(1)} v_h d\mathbf{z},$$

where $\mathbb{H}_h^{\varphi_y}(\Omega_1) := \left\{ u \in H_{\mathcal{B}_\#, \mathcal{B}_d}^1(\Omega_1) \mid u|_\tau \in \mathcal{P}_r(\tau) \forall \tau \in (\mathcal{T}_h \cap \Omega_1) \right\}$ with the same \mathcal{T}_h and r as for $\mathbb{H}_h(\Omega_L)$ (assuming Ω_1 -aligned elements).

3.2. Optimally Preconditioned Eigenvalue Algorithms. To solve the resulting discrete eigenvalue problem (3.2), we use the analytic results from section 2 to obtain the optimal shift as

$$(3.4) \quad \sigma = \lambda_\infty = \lim_{L \rightarrow \infty} \lambda_L^{(1)} = \lambda_{\varphi_y} \approx \lambda_h^{(1)},$$

by combining the results of Theorems 2.5 and 2.8. With the generalized Rayleigh quotient $R_{\mathbf{A}, \mathbf{B}}(\mathbf{x}) = (\mathbf{x}^T \mathbf{A} \mathbf{x}) / (\mathbf{x}^T \mathbf{B} \mathbf{x})$, we define:

DEFINITION 3.1 (Shifted Inverse Power Method, IP_σ). *Let $\mathbf{A}, \mathbf{B} \in \mathbb{R}^{n \times n}$ and a start vector $\mathbf{x}_0 \in \mathbb{R}^n$ be given, repeat*

$$(3.5) \quad \tilde{\mathbf{x}}_k = (\mathbf{A} - \sigma \mathbf{B})^{-1} \mathbf{B} \mathbf{x}_{k-1}, \quad \mathbf{x}_k = \tilde{\mathbf{x}}_k / \sqrt{\tilde{\mathbf{x}}_k^T \mathbf{B} \tilde{\mathbf{x}}_k}, \quad \lambda_k = R_{\mathbf{A}, \mathbf{B}}(\mathbf{x}_k),$$

until $\|\mathbf{A} \mathbf{x}_k - \lambda_k \mathbf{B} \mathbf{x}_k\|_2 < \tau_{tol}$ or $k > k_{max}$.

DEFINITION 3.2 (Locally Optimal Preconditioned Conjugate Gradient Method, LOPCG_σ). *Let $\mathbf{A}, \mathbf{B} \in \mathbb{R}^{n \times n}$, the preconditioner $P = (\mathbf{A} - \sigma \mathbf{B})^{-1}$, and the start vectors $\mathbf{x}_{-1}, \mathbf{x}_0 \in \mathbb{R}^n$ be given, repeat*

$$(3.6) \quad \begin{aligned} \mathbf{w}_k &= P(\mathbf{A} \mathbf{x}_{k-1} - R_{\mathbf{A}, \mathbf{B}}(\mathbf{x}_{k-1}) \mathbf{B} \mathbf{x}_{k-1}), \quad S_k = \text{span}(\{\mathbf{x}_{k-1}, \mathbf{w}_k, \mathbf{x}_{k-2}\}) \\ \tilde{\mathbf{x}}_k &= \arg \min_{\mathbf{y} \in S_k} R_{\mathbf{A}, \mathbf{B}}(\mathbf{y}), \quad \mathbf{x}_k = \tilde{\mathbf{x}}_k / \sqrt{\tilde{\mathbf{x}}_k^T \mathbf{B} \tilde{\mathbf{x}}_k}, \quad \lambda_k = R_{\mathbf{A}, \mathbf{B}}(\mathbf{x}_k), \end{aligned}$$

until $\|\mathbf{A} \mathbf{x}_k - \lambda_k \mathbf{B} \mathbf{x}_k\|_2 < \tau_{tol}$ or $k > k_{max}$.

In (3.6), the locally optimal step is calculated by minimizing in a 3-dimensional subspace with the standard Rayleigh–Ritz method [22] as $\tilde{\mathbf{x}}_k = \alpha_1 \mathbf{x}_{k-1} + \alpha_2 \mathbf{w}_k + \alpha_3 \mathbf{x}_{k-2}$, where the coefficients $\boldsymbol{\alpha} \in \mathbb{R}^3$ are derived from the smallest eigenpair solution of the 3-dimensional eigenvalue problem $\mathbf{V}^T \mathbf{A} \mathbf{V} \boldsymbol{\alpha} = \lambda^{(1)} \mathbf{V}^T \mathbf{B} \mathbf{V} \boldsymbol{\alpha}$ with $\mathbf{V} = [\mathbf{x}_{k-1} \ \mathbf{w}_k \ \mathbf{x}_{k-2}] \in \mathbb{R}^{n \times 3}$.

4. Numerical Experiments. This section concerns the numerical evaluation of the proposed eigensolver preconditioner. We implemented our method using the **Gridap** [21] framework in the Julia programming language [23]. **Gridap** turned out to be a very well-suited framework for our tests since it allowed us to quickly implement weak formulations in a high-level fashion, similar to the **FEniCS** [12, 55] framework in Python. For reproducibility, we provide all examples publicly in [54].

4.1. Homogenization of a Degenerate Eigenvalue Problem with Two Expanding Directions in Three Dimensions. Before we employ the optimal preconditioner for the linear Schrödinger eigenvalue problem (1.2), we first investigate the homogenization results of Theorem 2.8 since these results can be applied and studied independently. Thus, the theoretical predictions about the convergence of the m -dependent contribution $(u_{\mathcal{B}_d, \mathcal{B}_n, \rho, 0}^{(m)}, \lambda_{\mathcal{B}_d, \mathcal{B}_n, \rho, 0}^{(m)})$ in three dimensions ($p = 2, q = 1$) are studied numerically. We prescribe the weight function by

$$(4.1) \quad \rho(\mathbf{x}, \mathbf{y}) = \left(\sin(\pi y_1)^2 \left(10 \cos(\pi x_1)^2 + 10 \cos(\pi x_2)^2 + \frac{11}{10} - \sin(\pi y_1)^2 \right) \right)^2.$$

Note that we do not set $\rho = (\psi u_{y,1})$ as in Theorem 2.8 since we want to demonstrate the results for the more general case of ρ not being induced by eigenfunctions

but only satisfying the zero- and periodicity-condition on the boundary. The weight function ρ in (4.1) is positive a.e. and vanishing only on the \mathbf{y} -boundary. By construction, ρ is $[0, 1]^3$ -periodic and symmetric in the (x_1, x_2) -coordinates and thus fulfills all requirements of Theorem 2.8. We intentionally used the symmetry also to confirm the convergence of degenerate eigenpairs. For a better evaluation, we do not solve for Ω_L but solve an equivalent problem on the reference domain Ω_1 , where we factorized the $(1/L^2)$ -scaling (see Theorem 2.8) of the eigenvalue without affecting the eigenfunctions. To be precise, we check if the solution to

$$(4.2) \quad \begin{cases} -\nabla \cdot \left(\rho(L\mathbf{x}, \mathbf{y}) \operatorname{diag} \left(1, 1, \frac{1}{L^2} \right) \nabla u^{(m)} \right) = \nu^{(m)} \rho(L\mathbf{x}, \mathbf{y}) u^{(m)} & \text{in } (0, 1)^3 \\ u^{(m)} = 0 & \text{on } \{0, 1\}^2 \times (0, 1) \end{cases},$$

converge to $(u_0^{(m)}, \nu^{(m)})$ from (2.39) in the limit for $L \rightarrow \infty$. The calculation of this homogenized limit first needs the corrector functions to define the homogenized operators. Thus, we solve the corrector equation (2.41) using \mathbb{Q}_2 finite elements on a structured mesh with 30 intervals per direction. These corrector solutions allow the construction of the homogenized coefficients (according to (2.39) and (2.40)) with $\bar{D} \approx \operatorname{diag}(32.46332, 32.46332)$ and $\bar{C} \approx 48.91469$. We observe that $\bar{D}_{11} = \bar{D}_{22}$ as the result of choosing an (x_1, x_2) -symmetric weight function ρ . The homogenized diffusion matrix is diagonal since we have $\int_{\Omega_1} \nabla \cdot (\rho I) = 0$ by the divergence theorem as ρ defined by (4.1) is either periodic or zero on the boundary of the unit cube, which resembles the case of Remark 2.11. Therefore, we can solve the homogenized equation analytically (with the expressions from Remark 2.11) to obtain

$$(4.3) \quad \begin{aligned} \nu^{(1)} &= \frac{\pi^2 (1^2 \bar{D}_{11} + 1^2 \bar{D}_{22})}{\bar{C}} = \frac{2\pi^2 \bar{D}_{11}}{\bar{C}}, \quad \nu^{(2)} = \nu^{(3)} = \frac{5\pi^2 \bar{D}_{11}}{\bar{C}}, \quad \nu^{(4)} = \frac{8\pi^2 \bar{D}_{11}}{\bar{C}} \\ u_0^{(1)} &= \mathcal{N} \sin(\pi x_1) \sin(\pi x_2), \quad u_0^{(2)} = \mathcal{N} \sin(2\pi x_1) \sin(\pi x_2), \\ u_0^{(3)} &= \mathcal{N} \sin(\pi x_1) \sin(2\pi x_2), \quad u_0^{(4)} = \mathcal{N} \sin(2\pi x_1) \sin(2\pi x_2) \end{aligned}$$

with the normalization constant $\mathcal{N} = 2/\sqrt{\bar{C}} \approx 0.28596$ since

$$(4.4) \quad \left(\int_0^1 \sin^2(m_1 \pi x_1) dx_1 \right) \cdots \left(\int_0^1 \sin^2(m_p \pi x_p) dx_p \right) = 2^{-p/2} \quad \forall \mathbf{m} \in \mathbb{N}^p.$$

We then solve the eigenvalue problem (4.2) using the Galerkin method with \mathbb{Q}_2 elements and a structured partition of both expanding directions into $10L$ intervals. According to Theorem 2.8, the non-relevant third direction is only discretized with five partitions since it is not relevant in the limit. We solve the corresponding algebraic eigenvalue problem using a generalized inverse power method up to a tolerance of 10^{-8} for the residuals.

For the error comparison, we project the analytical solutions (4.3) into the corresponding subspace \mathbb{H}_h . Since $\nu^{(2)} = \nu^{(3)}$ by our construction of ρ , the corresponding eigenspace is two-dimensional, and the eigensolver returns some basis of this space. To resolve these spatial rotations and allow for an error comparison, we align the second and third eigenfunction by modifying their discrete eigenvectors with

$$(4.5) \quad \mathbf{x}_h^{(2)} = \langle \mathbf{x}_h^{(2)}, \mathbf{x}_0^{(2)} \rangle \mathbf{x}_h^{(2)} + \langle \mathbf{x}_h^{(3)}, \mathbf{x}_0^{(2)} \rangle \mathbf{x}_h^{(3)}, \quad \mathbf{x}_h^{(3)} = \langle \mathbf{x}_h^{(2)}, \mathbf{x}_0^{(3)} \rangle \mathbf{x}_h^{(2)} + \langle \mathbf{x}_h^{(3)}, \mathbf{x}_0^{(3)} \rangle \mathbf{x}_h^{(3)},$$

where $\mathbf{x}_0^{(m)}$ denote the exact eigenvectors. The resulting discrete eigenfunctions $u_h^{(m)}$ for $m = 1, 2, 3, 4$ are visualized in Figure 4 for $L \in \{2^1, \dots, 2^4\}$ together with the

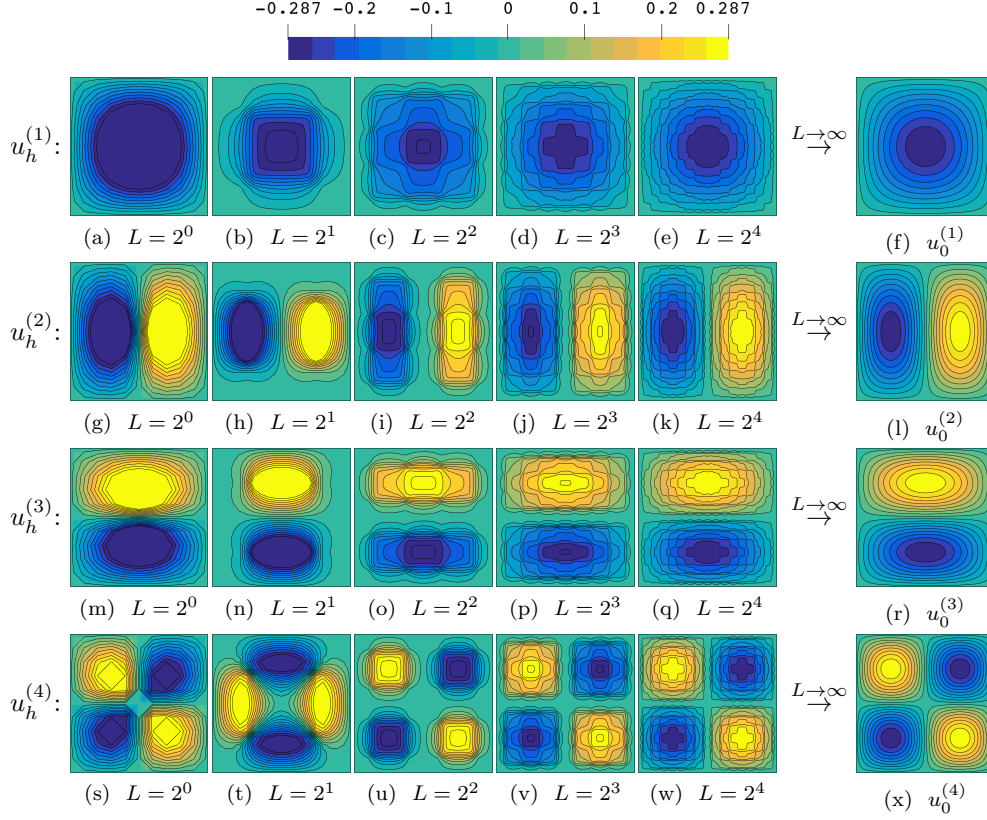


FIG. 4. The first four calculated eigenfunctions of the eigenvalue homogenization problem (4.2) converge weakly for $L \rightarrow \infty$ to the solutions of the homogenized equation. The figure presents two-dimensional cut-planes through the middle of the domain at $y_1 = 1/2$.

corresponding homogenized solutions $u_0^{(m)}$. We can observe that for larger domain lengths L , the eigenfunctions converge to their corresponding limits if we would neglect the oscillatory isolines that indicate strong gradients. This observation corresponds to our theoretical results that the convergence is only weak when we consider the $H^1(\Omega_1)$ -norm. To quantify the convergence, we evaluate the $L^2(\Omega_1)$ -error of the eigenfunctions and the eigenvalue error in Figure 5. We measure a first-order converge for the L^2 -error and a second-order converge for the eigenvalues. This observation matches the theoretical results from subsection 2.3 since we proved strong convergence in L^2 of the eigenfunctions and convergence of the eigenvalues to $\nu^{(m)}$. We also examine the ratio of the eigenvalues $\lambda^{(m)}/\lambda^{(m+1)}$ in Figure 5, where the degeneracy of $m = 2$, a monotonic decrease for $m = 3$, and a pre-asymptotic effect for $m = 1$ is visible. This observation confirms the prediction of Corollary 2.10 that the fundamental ratio can only be uniformly bounded for all $L > L^*$ when pre-asymptotic effects have vanished.

4.2. Using the Optimal Shift-And-Invert Preconditioner. To show the practical advantage of using the optimal preconditioning technique of subsection 3.2, we compare the convergence histories of the IP and LOPCG method for the cases of no shift ($\sigma = 0$), a good shift ($\sigma = 0.99\lambda_\infty$), and the optimal shift ($\sigma = \lambda_\infty$). The optimal shift $\lambda_\infty = \lambda_{\mathcal{B}_\#, \mathcal{B}_{d,1}, V}^{(1)}(\Omega_1)$ is obtained in $\mathcal{O}(1)$ since the domain Ω_1 is fixed. We then

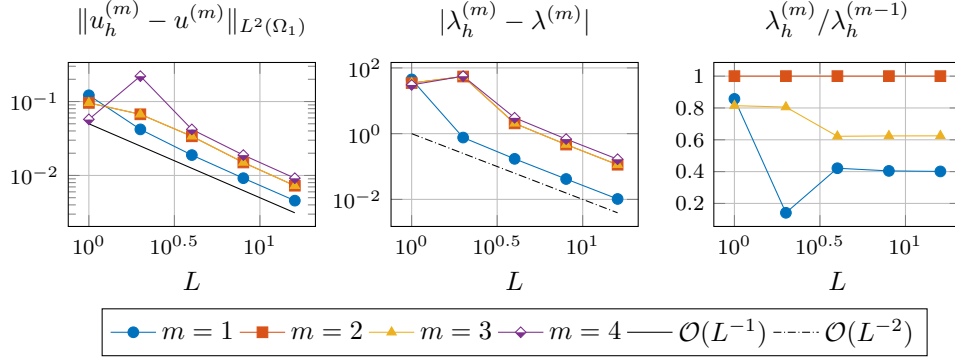


FIG. 5. Errors between the solution of (4.2) and the corresponding homogenized limit: We can observe the first-order convergence for all eigenfunctions in the L^2 -norm and the second-order convergence for the eigenvalues. The ratios between two adjacent eigenvalues reveal a degenerate state and a non-monotonic convergence for the fundamental ratio $\lambda_h^{(1)}/\lambda_h^{(2)}$.

aim to solve (1.2) on Ω_L for $\ell = 1$ and increasing L . The calculations use \mathbb{P}_1 finite elements on a regular tetrahedral mesh with mesh size $h = 1/100$ and the periodic potential $V(x, y) = 10^2 \sin(\pi x)^2 \sin(\pi y)^2$. We chose the start vectors $\mathbf{x}_0 = \mathbf{1}, \mathbf{x}_{-1} = \mathbf{e}_1$. The solvers aim to reduce the spectral residual $\mathbf{r}_k = \mathbf{A}\mathbf{x}_k - \mathbf{R}_{\mathbf{A}, \mathbf{B}}(\mathbf{x}_k)\mathbf{B}\mathbf{x}_k$ below the tolerance $\tau_{\text{tol}} = 10^{-10}$ and stop after 100 iterations.

The results in Figure 6 indicate the drastic reduction in convergence speed for the unshifted algorithms. For the case of optimal preconditioning, both eigensolvers only need a couple of iterations to converge, as predicted by Theorem 2.9. When applying a good but not optimal shift of $0.99\lambda_\infty$, fast convergence rates for lower values of L can be observed. However, the convergence also deteriorates in the asymptotic limit of $L \rightarrow \infty$. This fact underlines the requirement for σ to be the exact asymptotic limit if the method shall provide convergence in a fixed number of iterations for all possible L . Furthermore, all three cases show a faster convergence of the LOPCG compared to the IP method.

4.3. Extension to Complex Domains: Barrier Principle and Defects in x -Direction. The initial box setup of $\Omega_L = (0, L)^p \times (0, \ell)^q$ from section 1 is very suitable for the mathematical analysis performed in section 2. However, for practical applications, we need to generalize the theory to more realistic domains. Luckily, this can be quite intuitively done with some simple considerations.

Consider, for example, the setup of Figure 7, in which one aims to simulate a union of three disks $\tilde{\Omega} = \bigcup_{i=1}^3 B_R((R + 2(i-1)r, 0)^T) = \tilde{\Omega}_l \cup \left(\bigcup_{i=1}^3 \tilde{\Omega}_i\right) \cup \tilde{\Omega}_r$ where $B_R(\mathbf{p})$ denotes a disk with radius R centered at \mathbf{p} and $r = R - d$ with the overlap d . These disks are all aligned along the x -axis and have a fixed overlap. We define the rectangular unit cell as the box with side lengths $\{2r, 2R\}$, where one disk is contained entirely. Inside this unit cell, we assume the potential as directional periodic. Furthermore, we have domain defects $\tilde{\Omega}_l$ and $\tilde{\Omega}_r$ that are not part of any unit cell on the left and the right side. In this setup, two problems arise – the simulation of non-box-shaped domains and the handling of domain defects.

4.3.1. Barrier Principle for an Optical Lattice Potential. To overcome the first issue, we could simulate the whole domain $\Omega_{L=6r+2d}$. However, we are only

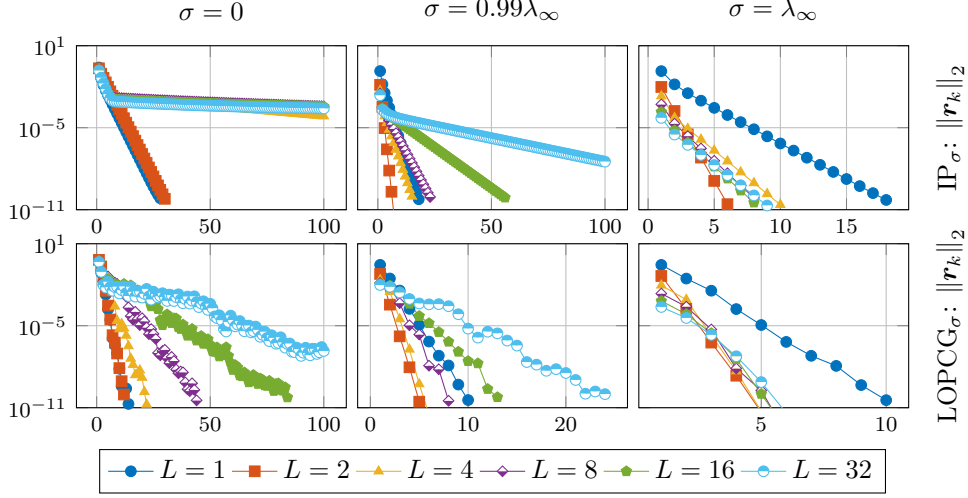


FIG. 6. A comparison of the IP_σ and $LOPCG_\sigma$ for the cases of $\sigma = 0$, $\sigma = 0.99\lambda_\infty$, and $\sigma = \lambda_\infty$ for different domain lengths L .

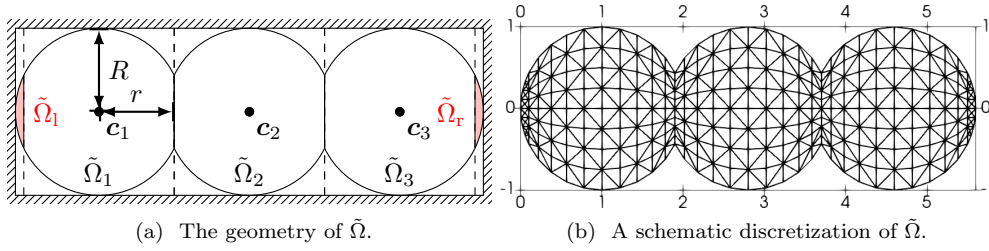


FIG. 7. A union of three disks ($R = 1$) domain with defects in the x -direction and overlap of $d = 0.1$: The whole domain $\tilde{\Omega}$ comprises three identical base cells $\tilde{\Omega}_i$ and two domain defects $\tilde{\Omega}_l, \tilde{\Omega}_r$.

interested in the union of disks domain $\tilde{\Omega}$, and a prescription of Dirichlet values on $\partial\tilde{\Omega}$ might be problematic since it is inside the domain. It is well known that we can simply modify the potential V to achieve this setting. To avoid nontrivial values of ϕ_L in certain regions, we can apply a significant penalty term to V . We call this strategy the *barrier principle*, which extends a given potential V to the barrier potential $\tilde{V}(\mathbf{z}; V, a) = V(\mathbf{z}) + a\chi_{\tilde{\Omega}^c}(\mathbf{z})$ where $a \geq 0$ is a penalty term, and $\chi_{\tilde{\Omega}^c}$ is the indicator function for the complement of $\tilde{\Omega}$. For an increasing value of $a \rightarrow \infty$, we can still apply our theory for any finite value of a . In the limit case, the eigenvalue problem on the box-shaped domain Ω_{6r+2d} is equivalent to an eigenvalue problem, purely posed on the subdomain $\tilde{\Omega} \subset \Omega_{6r+2d}$.

To demonstrate the barrier effect of $\tilde{V}(\mathbf{z}; V, a)$, we inspect the union of three disks case from Figure 7 in combination with the optical lattice potential [43]

$$(4.6) \quad V(x, y) = 100 \left(1 - \sin \frac{\omega\pi(x-d)}{2(R-d)} \sin \frac{\omega\pi(y-(R-d))}{2(R-d)} \right),$$

where $\omega = 9, R = 1, d = 0.1$ for various penalty terms $a \in \{2^0, 2^5, \dots, 2^{20}\}$. Figure 8 shows the first eigenfunction, which is calculated with the $LOPCG_{\sigma=0}$ method for

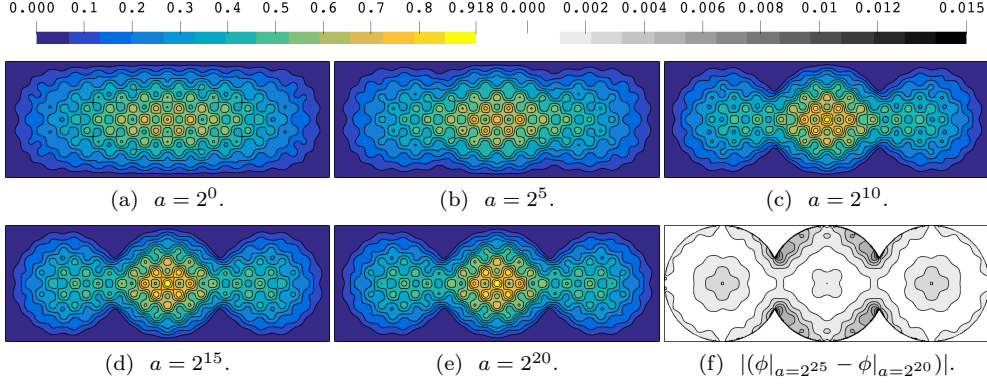


FIG. 8. Effect of Barrier Potential $\tilde{V}(\mathbf{z}; 0, a)$ for varying penalty parameters a in the union of disks domain $\tilde{\Omega}$ of Figure 7. With increasing a , the resulting problem statement reduces to the eigenproblem formulated in $\tilde{\Omega}$. When comparing the change between $a = 2^{15}$ and $a = 2^{20}$ in Figure 8f, the solution's overall change is small and focussed on the connection points. Also, we see an interpolation error at the disk boundary since the underlying mesh is not boundary-aligned.

$\tau_{\text{tol}} = 10^{-10}$ on a structured \mathbb{Q}_1 -mesh with $h = 1/100$. It can be observed that with a increasing, the eigenfunction outside of $\tilde{\Omega}$ approaches zero.

However, these above considerations are purely theoretical. In practice, we directly exclude the regions $\Omega_{6r+2d} \setminus \tilde{\Omega}$ and purely solve and mesh on $\tilde{\Omega}$ as displayed in Figure 7b.

4.3.2. Principle of Defect Invariance. When it comes to simulating the union of disk domain of subsection 4.3 with the optimally preconditioned eigensolver, we also need to calculate the shift $\sigma = \lambda_\infty$. For domains without any domain defect that perfectly match the potential's period, this is done by simulating one unit cell Ω_1 with Dirichlet zero in \mathbf{y} - and periodic boundary conditions in \mathbf{x} -direction as theoretically derived in Theorems 2.5 and 2.8.

For the case of defects located at the extremities of the expanding \mathbf{x} -direction as a subset of an imaginary unit cell Ω_1 , we can do the same (if the potential acts as usual in the defect regions). The limit eigenvalue does not change since we can prove:

THEOREM 4.1 (Principle of Defect Invariance). *Let $\Omega_{L+2\delta}$ with L denoting the \mathbf{x} -period of the potential V and $\delta < L$ be given. For the linear Schrödinger eigenvalue problem (1.2) posed on $\Omega_{L+2\delta}$, it still holds that $\lim_{L \rightarrow \infty} \lambda_L^{(m)} = \lambda_{\varphi_y}$.*

Proof. Consider $\Omega_L \subset \Omega_{L+2\delta} \subset \Omega_{L+2}$. Then, by the inclusion principle [44, p13] for elliptic operators with Dirichlet boundary conditions, we have

$$(4.7) \quad \lambda_{\mathcal{B}_d, \mathcal{B}_d, 0, V}^{(m)}(\Omega_L) \leq \lambda_{\mathcal{B}_d, \mathcal{B}_d, 0, V}^{(m)}(\Omega_{L+2\delta}) \leq \lambda_{\mathcal{B}_d, \mathcal{B}_d, 0, V}^{(m)}(\Omega_{L+2})$$

Using the factorizations of Theorem 2.5, this is equivalent to

$$(4.8) \quad \lambda_{\varphi_y}^{(1)}(\Omega_L) + \lambda_{u_{y,2}}^{(m)}(\Omega_L) \leq \lambda_{\mathcal{B}_d, \mathcal{B}_d, 0, V}^{(m)}(\Omega_{L+2\delta}) \leq \lambda_{\varphi_y}^{(1)}(\Omega_{L+2}) + \lambda_{u_{y,2}}^{(m)}(\Omega_{L+2}).$$

Since $\lambda_{\varphi_y}^{(1)}(\Omega_L) = \lambda_{\varphi_y}^{(1)}(\Omega_{L+2}) = \lambda_{\varphi_y}^{(1)}(\Omega_1)$ and $\lambda_{u_{y,2}}^{(m)}(\Omega_L), \lambda_{u_{y,2}}^{(m)}(\Omega_{L+2}) \in \mathcal{O}(1/L^2)$ by Theorem 2.8, we have by the Sandwich Lemma that

$$(4.9) \quad \lim_{L \rightarrow \infty} \lambda_{\mathcal{B}_d, \mathcal{B}_d, 0, V}^{(m)}(\Omega_{L+2\delta}) = \lambda_{\varphi_y}^{(1)}(\Omega_1). \quad \square$$

With that knowledge, we are prepared to solve the union of disks geometry in the next subsection 4.4.

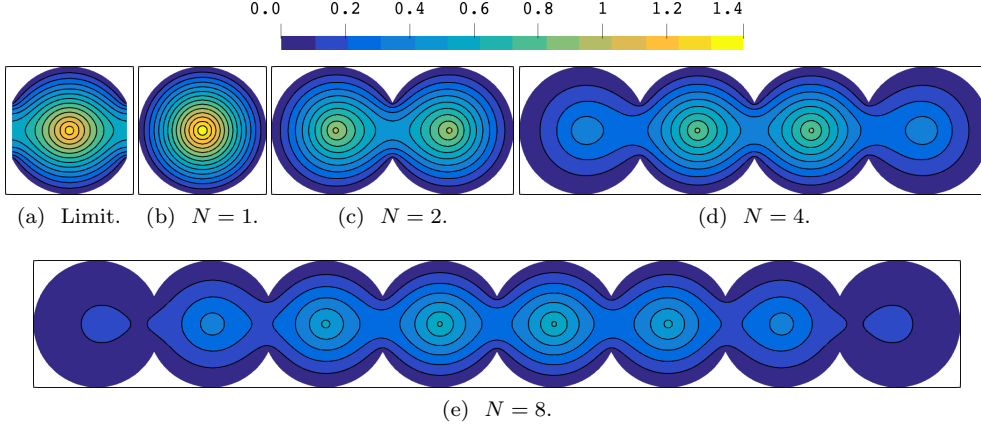


FIG. 9. Contours of the first eigenfunction for the union of N disks using the truncated Coulomb potential without long-range interactions: Figure 9a shows the asymptotic limit eigenfunction with periodic boundary conditions in x -direction.

4.4. Chain Model with Truncated Coulomb Potential in Two Dimensions. Consider the domain $\tilde{\Omega}_N = \bigcup_{i=1}^N B_R \left((R + 2(i-1)r, 0)^T \right)$ with the parameters $R = 1, r = 0.9$. Chain-like molecules in the context of molecular simulations inspire this model. For real applications, the potential is a Coulomb-potential. Since a singularity of V violates the assumption (A2), we use a truncated Coulomb potential

$$(4.10) \quad V_{\text{C,lim}}(\mathbf{z}; b) = \begin{cases} -\frac{Z}{\|\mathbf{z}\|_2} & \text{for } \|\mathbf{z}\|_2 \geq b \\ -\frac{Z}{b} & \text{for } \|\mathbf{z}\|_2 < b \end{cases},$$

to mimic, e.g., the electrostatic potential with charge $Z > 0$. We also have to neglect long-range interaction to fulfill the periodicity assumption on V . Consider the N centers $\{\mathbf{c}_i\}_{i=1}^N$ with $\mathbf{c}_i = (R + (i-1)2r, 0)$. We prescribe the compound periodic potential

$$(4.11) \quad V(\mathbf{z}) = \sum_{i \in \{i: |\mathbf{z} - \tilde{\mathbf{c}}_i| < R\}} V_{\text{C,lim}}(\mathbf{z} - \tilde{\mathbf{c}}_i; b),$$

where $\tilde{\mathbf{c}}_i \in \{\mathbf{c}_i\}_{i=1}^N \cup \{\mathbf{c}_1 - (2r, 0)\} \cup \{\mathbf{c}_N + (2r, 0)\}$ include ghost centers to fulfill the periodicity assumption (A1) also in the defect regions. We also note that the semi-positivity assumption (A3) is violated. However, it turned out that the resulting spectrum is still positive, the operator, thus, elliptic, and our theory is applicable. Nevertheless, it would also be possible to simply shift the potential to positive values without affecting the results.

A series of computations for $N = 1, 2, 4, \dots, 32$ is performed using the LOPCG $_{\sigma}$ method for the potential parameters $Z = 1, b = 10^{-4}$ and the tolerance $\tau_{\text{tol}} = 10^{-10}$. The spatial discretization uses unstructured \mathbb{P}_1 elements, symmetrically meshed, as shown in Figure 7b. The optimal shift calculation uses the unit cell $\tilde{\Omega}_0 = \tilde{\Omega}_1 \cap [R - r, R - r] \times [-R, R]$ with periodic boundary conditions in x -direction and zero boundary conditions on the rest. Thus, $\sigma = \lambda_{\varphi_y}(\tilde{\Omega}_0) \approx 1.08784$ can be computed a priori in $\mathcal{O}(1)$ since the unit cell is independent of N .

In Figure 9, the resulting ground state eigenfunctions $\phi_h^{(1)}$ are presented with the solution to the base problem in Figure 9a. We can observe for increasing N that

TABLE 1

The summary of computations for the union of N disks with the truncated Coulomb potential. Due to the same discretization density, the number of nodes n_{nodes} for each mesh is approximately proportional to the number of disks N (up to the defects). The wall times are measured on an Intel X7542 CPU using one core.

$N \propto L$	n_{nodes}	$\lambda_h^{(1)}$	$\max \phi_h^{(1)}$	k_{it}	$\frac{\lambda_{\max}(\mathbf{A}-\sigma\mathbf{B})}{\lambda_{\min}(\mathbf{A}-\sigma\mathbf{B})}$	$t_{\text{eig}} [s]$	$\frac{t_{\text{eig}}}{N} [s]$
1	89,869	1.96222	1.44	5	$4.83 \cdot 10^5$	1.83	1.83
2	$1.69 \cdot 10^5$	1.46912	0.96	5	$1.25 \cdot 10^6$	3.95	1.97
4	$3.27 \cdot 10^5$	1.20013	0.85	5	$4.25 \cdot 10^6$	7.7	1.92
8	$6.44 \cdot 10^5$	1.11768	0.64	5	$1.14 \cdot 10^7$	17.03	2.13
16	$1.28 \cdot 10^6$	1.0955	0.46	5	$2.55 \cdot 10^7$	33.06	2.07
32	$2.54 \cdot 10^6$	1.08978	0.33	5	$5.33 \cdot 10^7$	64.96	2.03

the solution inside a single disk approaches the shape of the solution to the unit cell problem. This convergence is the expected behavior, as it was shown theoretically in [section 2](#). In [Table 1](#), we observe that, due to the optimal preconditioning, the number of iterations needed to meet the required residual tolerance is of order $\mathcal{O}(1)$. Furthermore, the method shows a linearly scaling behavior since the ratio of calculation time to the disk amount t_{eig}/N seems to be independent of N .

4.5. Plane Model with Kronig–Penney Potential in Three Dimensions.

Finally, we also show the preconditioner’s optimality for a three-dimensional case with two expanding directions ($p = 2, q = 1$). For this example, we use a three-dimensional Kronig–Penney potential [\[57\]](#), defined by

$$(4.12) \quad V(\mathbf{z}) = \begin{cases} 0 & \text{for } \|\mathbf{z} \bmod \mathbf{1} - \mathbf{1}/2\|_1 < 1/4, \\ 100 & \text{else} \end{cases},$$

where $\mathbf{1}$ denotes the vector of ones in d dimensions. This potential represents cubic wells with sidelength 0.5 centered in the unit cubes, which form the plane-like expanding domain $\Omega_L = (0, L)^2 \times (0, 1)$ with $L \in \mathbb{N}$. We again calculate the optimal shift $\sigma = \lambda_{\mathcal{B}_{\#}, \mathcal{B}_d, \mathbf{1}, V}^{(1)}$ on the unit cube and use it to precondition the Ω_L -problem. Finally, both problems are discretized using a uniform mesh size of $h = 1/10$ and \mathbb{Q}_2 elements resulting in $\sigma \approx 57.60485$. We use the LOPCG $_{\sigma}$ with $\tau_{\text{tol}} = 10^{-10}$ and solve for the ground state solution. The simulations are performed on a series of domains Ω_L with $L \in \{1, 2, 4, \dots, 32\}$. In [Table 2](#), we observe that the number of eigensolver iterations k_{it} does not increase for $L \rightarrow \infty$, confirming our theory. However, in contrast to [Table 1](#), a slight increase in solution time per number of unit cells (t_{eig}/L^2) can be observed. This increase is the expected behavior of using a direct solver for sparse matrices with increased bandwidth for $L \rightarrow \infty$ for our case of $p = 2$ expanding directions.

5. Conclusion. This work presented an optimal shift-and-invert preconditioner to solve the linear periodic Schrödinger eigenvalue problem in a constant number of eigensolver iterations for domains expanding periodically in a subset of directions. We analyzed and proved the optimality of the method using factorization and homogenization techniques. The analysis revealed powerful insights on the behavior of the eigenfunctions and eigenvalues. Significantly, the representation of the searched eigenfunction as the product of easy-to-calculate functions leads to a decisive result – the

TABLE 2

The summary of computations for the plane-like expanding domain in three directions with the Kronig–Penney potential. The number of unit cells N now scales quadratically with L .

L	n_{nodes}	$\lambda_h^{(1)}$	$\max \phi_h^{(1)}$	k_{it}	$t_{\text{eig}} [s]$	$\frac{t_{\text{eig}}}{L^2} [s]$
1	1,331	58.99915	4.71	5	0.16	0.16
2	4,851	58.30881	2.31	6	0.52	0.13
4	18,491	57.81186	1.95	6	3.01	0.19
8	72,171	57.6587	1.09	7	15.28	0.24
16	$2.85 \cdot 10^5$	57.61845	0.56	7	73.33	0.29
32	$1.13 \cdot 10^6$	57.60826	0.28	6	320.64	0.31

corresponding eigenvalues can be expressed as the sum of other eigenvalues, which can be much easier computed in practice than solving the whole system. This realization makes the proposed method very practical since calculating the optimal shift can be done in $\mathcal{O}(1)$. We then extended the results to complex and defect domains shapes to allow for a broader range of geometrical applications. Finally, in our experiments, we showed the practical usability of the method for chain-like and plane-like expanding domains.

Limitations of our method include the assumptions on the potential V to be essentially bounded and periodic. Also, we observed that using the perfect shift in the eigensolver algorithms leads naturally to an ill-conditioned system matrix $(\mathbf{A} - \sigma \mathbf{B})$. Thus, future work could weaken the periodicity assumptions on V by, e.g., allowing for a perturbation of δV , that vanishes in the limit $L \rightarrow \infty$. Also, efficient preconditioners for the linear system involving $(\mathbf{A} - \sigma \mathbf{B})$ must be constructed when the system size requires iterative linear solvers.

REFERENCES

- [1] P. M. AJAYAN AND O. Z. ZHOU, *Applications of Carbon Nanotubes*, in Carbon Nanotubes: Synthesis, Structure, Properties, and Applications, M. S. Dresselhaus, G. Dresselhaus, and P. Avouris, eds., Topics in Applied Physics, Springer, Berlin, Heidelberg, 2001, pp. 391–425, https://doi.org/10.1007/3-540-39947-X_14.
- [2] G. ALLAIRE, *Dispersive limits in the homogenization of the wave equation*, Annales de la faculté des sciences de Toulouse Mathématiques, 12 (2003), pp. 415–431, <https://doi.org/10.5802/afst.1055>.
- [3] G. ALLAIRE, *Numerical Analysis and Optimization: An Introduction to Mathematical Modelling and Numerical Simulation*, Numerical Mathematics and Scientific Computation, Oxford University Press, 2007.
- [4] G. ALLAIRE, *A brief introduction to homogenization and miscellaneous applications*, ESAIM: Proceedings, 37 (2012), pp. 1–49, <https://doi.org/10.1051/proc/201237001>.
- [5] G. ALLAIRE AND G. BAL, *Homogenization of the criticality spectral equation in neutron transport*, ESAIM: Mathematical Modelling and Numerical Analysis, 33 (1999), pp. 721–746, <https://doi.org/10.1051/m2an:1999160>.
- [6] G. ALLAIRE AND Y. CAPDEBOSCQ, *Homogenization of a spectral problem in neutronic multi-group diffusion*, Computer Methods in Applied Mechanics and Engineering, 187 (2000), pp. 91–117, [https://doi.org/10.1016/S0045-7825\(99\)00112-7](https://doi.org/10.1016/S0045-7825(99)00112-7).
- [7] G. ALLAIRE AND Y. CAPDEBOSCQ, *Homogenization and localization for a 1-D eigenvalue problem in a periodic medium with an interface*, Annali di Matematica Pura ed Applicata, 181 (2002), pp. 247–282, <https://doi.org/10.1007/s102310100040>.
- [8] G. ALLAIRE AND C. CONCA, *Bloch wave homogenization and spectral asymptotic analysis*, Journal de Mathématiques Pures et Appliquées, 77 (1998), pp. 153–208, [https://doi.org/10.1016/S0021-7824\(98\)80068-8](https://doi.org/10.1016/S0021-7824(98)80068-8).
- [9] G. ALLAIRE AND F. MALIGE, *Analyse asymptotique spectrale d’un problème de diffusion neu-*

- tronique, Comptes Rendus de l'Académie des Sciences - Series I - Mathematics, 324 (1997), pp. 939–944, [https://doi.org/10.1016/S0764-4442\(97\)86972-8](https://doi.org/10.1016/S0764-4442(97)86972-8).
- [10] G. ALLAIRE AND A. PIATNITSKI, *Uniform spectral asymptotics for singularly perturbed locally periodic operators*, Communications in Partial Differential Equations, 27 (2002), pp. 705–725, <https://doi.org/10.1081/PDE-120002871>.
 - [11] G. ALLAIRE AND A. PIATNITSKI, *Homogenization of the Schrödinger Equation and Effective Mass Theorems*, Communications in Mathematical Physics, 258 (2005), pp. 1–22, <https://doi.org/10.1007/s00220-005-1329-2>.
 - [12] M. ALNÆS, J. BLECHTA, J. HAKE, A. JOHANSSON, B. KEHLET, A. LOGG, C. RICHARDSON, J. RING, M. E. ROGNES, AND G. N. WELLS, *The FEniCS Project Version 1.5*, Archive of Numerical Software, 3 (2015), <https://doi.org/10.11588/ans.2015.100.20553>.
 - [13] R. ALTMANN, P. HENNING, AND D. PETERSEIM, *Localization and delocalization of ground states of Bose-Einstein condensates under disorder*, June 2020, <https://arxiv.org/abs/2006.00773>.
 - [14] R. ALTMANN, P. HENNING, AND D. PETERSEIM, *Quantitative Anderson localization of Schrödinger eigenstates under disorder potentials*, Mathematical Models and Methods in Applied Sciences, 30 (2020), pp. 917–955, <https://doi.org/10.1142/S0218202520500190>.
 - [15] R. ALTMANN, P. HENNING, AND D. PETERSEIM, *The J-method for the Gross-Pitaevskii eigenvalue problem*, Numerische Mathematik, 148 (2021), pp. 575–610, <https://doi.org/10.1007/s00211-021-01216-5>.
 - [16] R. ALTMANN AND D. PETERSEIM, *Localized Computation of Eigenstates of Random Schrödinger Operators*, SIAM Journal on Scientific Computing, 41 (2019), pp. B1211–B1227, <https://doi.org/10.1137/19M1252594>.
 - [17] X. ANTOINE AND R. DUBOSCQ, *GPELab, a Matlab toolbox to solve Gross-Pitaevskii equations I: Computation of stationary solutions*, Computer Physics Communications, 185 (2014), pp. 2969–2991, <https://doi.org/10.1016/j.cpc.2014.06.026>.
 - [18] X. ANTOINE AND R. DUBOSCQ, *GPELab, a Matlab toolbox to solve Gross-Pitaevskii equations II: Dynamics and stochastic simulations*, Computer Physics Communications, 193 (2015), pp. 95–117, <https://doi.org/10.1016/j.cpc.2015.03.012>.
 - [19] X. ANTOINE, A. LEVITT, AND Q. TANG, *Efficient spectral computation of the stationary states of rotating Bose-Einstein condensates by the preconditioned nonlinear conjugate gradient method*, Journal of Computational Physics, 343 (2017), pp. 92–109, <https://doi.org/10.1016/j.jcp.2017.04.040>.
 - [20] I. BABUŠKA AND J. E. OSBORN, *Finite Element-Galerkin Approximation of the Eigenvalues and Eigenvectors of Selfadjoint Problems*, Mathematics of Computation, 52 (1989), p. 24.
 - [21] S. BADIA AND F. VERDUGO, *Gridap: An extensible Finite Element toolbox in Julia*, Journal of Open Source Software, 5 (2020), p. 2520, <https://doi.org/10.21105/joss.02520>.
 - [22] Z. BAI, J. DEMMEL, J. DONGARRA, A. RUHE, AND H. VAN DER VORST, eds., *Templates for the Solution of Algebraic Eigenvalue Problems: A Practical Guide*, Society for Industrial and Applied Mathematics, Jan. 2000, <https://doi.org/10.1137/1.9780898719581>.
 - [23] J. BEZANSON, A. EDELMAN, S. KARPINSKI, AND V. B. SHAH, *Julia: A Fresh Approach to Numerical Computing*, SIAM Review, 59 (2017), pp. 65–98, <https://doi.org/10.1137/141000671>.
 - [24] H. BREZIS, *Functional Analysis, Sobolev Spaces and Partial Differential Equations*, Springer New York, New York, NY, 2010, <https://doi.org/10.1007/978-0-387-70914-7>.
 - [25] E. CANCÈS, G. KEMLIN, AND A. LEVITT, *Convergence Analysis of Direct Minimization and Self-Consistent Iterations*, SIAM Journal on Matrix Analysis and Applications, 42 (2021), pp. 243–274, <https://doi.org/10.1137/20M1332864>.
 - [26] S. CARR, D. MASSATT, S. B. TORRISI, P. CAZEAUX, M. LUSKIN, AND E. KAXIRAS, *Relaxation and domain formation in incommensurate two-dimensional heterostructures*, Physical Review B, 98 (2018), pp. 224102–1–224102–7, <https://doi.org/10.1103/PhysRevB.98.224102>.
 - [27] P. CAZEAUX, M. LUSKIN, AND D. MASSATT, *Energy Minimization of Two Dimensional Incommensurate Heterostructures*, Archive for Rational Mechanics and Analysis, 235 (2020), pp. 1289–1325, <https://doi.org/10.1007/s00205-019-01444-y>.
 - [28] M. CHIPOT, *On some anisotropic singular perturbation problems*, Asymptotic Analysis, (2007), p. 21, <https://doi.org/10.5167/uzh-21524>.
 - [29] M. CHIPOT, *L goes to plus infinity: An update*, Journal of the Korean Society for Industrial and Applied Mathematics, 18 (2014), pp. 107–127, <https://doi.org/10.12941/JKSIAM.2014.18.107>.
 - [30] M. CHIPOT, A. ELFANNI, AND A. ROUGIREL, *Eigenvalues, Eigenfunctions in Domains Becoming Unbounded*, in Hyperbolic Problems and Regularity Questions, M. Padula and L. Zanghirati, eds., Birkhäuser Basel, Basel, 2007, pp. 69–78, <https://doi.org/10.1007/>

- 978-3-7643-7451-8.8.
- [31] M. CHIPOT, W. HACKBUSCH, S. SAUTER, AND A. VEIT, *Numerical Approximation of Poisson Problems in Long Domains*, Vietnam Journal of Mathematics, (2021), <https://doi.org/10.1007/s10013-021-00512-9>.
 - [32] M. CHIPOT AND A. ROUGIREL, *On the asymptotic behaviour of the solution of elliptic problems in cylindrical domains becoming unbounded*, Communications in Contemporary Mathematics, 04 (2002), pp. 15–44, <https://doi.org/10.1142/S0219199702000555>.
 - [33] M. CHIPOT AND A. ROUGIREL, *On the asymptotic behaviour of the eigenmodes for elliptic problems in domains becoming unbounded*, Transactions of the American Mathematical Society, 360 (2008), pp. 3579–3603, <https://doi.org/10.1090/S0002-9947-08-04361-4>.
 - [34] M. CHIPOT, P. ROY, AND I. SHAFRIR, *Asymptotics of eigenstates of elliptic problems with mixed boundary data on domains tending to infinity*, Asymptotic Analysis, 85 (2013), pp. 199–227, <https://doi.org/10.3233/ASY-131182>.
 - [35] M. CHIPOT AND Y. XIE, *On the asymptotic behaviour of elliptic problems with periodic data*, Comptes Rendus Mathématique, 339 (2004), pp. 477–482, <https://doi.org/10.1016/j.crma.2004.09.007>.
 - [36] R. COURANT AND D. HILBERT, *Methods of Mathematical Physics. Volume I*, Wiley, New York, 1989, <https://doi.org/10.1002/9783527617210>.
 - [37] R. DONG, D. LI, AND L. WANG, *Regularity of elliptic systems in divergence form with directional homogenization*, Discrete & Continuous Dynamical Systems - A, 38 (2018), pp. 75–90, <https://doi.org/10.3934/dcds.2018004>.
 - [38] R. DONG, D. LI, AND L. WANG, *Directional homogenization of elliptic equations in non-divergence form*, Journal of Differential Equations, 268 (2020), pp. 6611–6645, <https://doi.org/10.1016/j.jde.2019.11.041>.
 - [39] M. A. FREITAG AND A. SPENCE, *Convergence of inexact inverse iteration with application to preconditioned iterative solves*, BIT Numerical Mathematics, 47 (2007), pp. 27–44, <https://doi.org/10.1007/s10543-006-0100-1>.
 - [40] M. GALEWSKI, B. GALEWSKA, AND E. SCHMEIDEL, *Conditions for having a diffeomorphism between two Banach spaces*, Electronic Journal of Differential Equations, 99 (2014), pp. 1–6.
 - [41] D. GILBARG AND N. S. TRUDINGER, *Elliptic Partial Differential Equations of Second Order*, Classics in Mathematics, Springer-Verlag, Berlin Heidelberg, second ed., 2001, <https://doi.org/10.1007/978-3-642-61798-0>.
 - [42] P. HEID, B. STAMM, AND T. P. WIHLE, *Gradient flow finite element discretizations with energy-based adaptivity for the Gross-Pitaevskii equation*, Journal of Computational Physics, 436 (2021), p. 110165, <https://doi.org/10.1016/j.jcp.2021.110165>.
 - [43] P. HENNING AND D. PETERSEIM, *Sobolev Gradient Flow for the Gross-Pitaevskii Eigenvalue Problem: Global Convergence and Computational Efficiency*, SIAM Journal on Numerical Analysis, 58 (2020), pp. 1744–1772, <https://doi.org/10.1137/18M1230463>.
 - [44] A. HENROT, *Extremum Problems for Eigenvalues of Elliptic Operators*, Frontiers in Mathematics, Birkhäuser Basel, 2006, <https://doi.org/10.1007/3-7643-7706-2>.
 - [45] M. F. HERBST AND A. LEVITT, *Black-box inhomogeneous preconditioning for self-consistent field iterations in density functional theory*, Journal of Physics: Condensed Matter, 33 (2021), p. 085503, <https://doi.org/10.1088/1361-648X/abcdbd>.
 - [46] V. V. JIKOV, S. M. KOZLOV, AND O. A. OLEINIK, *Homogenization of Differential Operators and Integral Functionals*, Springer-Verlag, Berlin Heidelberg, 1994, <https://doi.org/10.1007/978-3-642-84659-5>.
 - [47] S. KESAVAN, *Homogenization of elliptic eigenvalue problems: Part 1*, Applied Mathematics and Optimization, 5 (1979), pp. 153–167, <https://doi.org/10.1007/BF01442551>.
 - [48] S. KESAVAN, *Homogenization of elliptic eigenvalue problems: Part 2*, Applied Mathematics and Optimization, 5 (1979), pp. 197–216, <https://doi.org/10.1007/BF01442554>.
 - [49] A. KUTNER AND A.-M. SÄNDIG, *Some Applications of Weighted Sobolev Spaces*, vol. 100 of Teubner-Texte Zur Mathematik, Vieweg+Teubner Verlag, Wiesbaden, 1987, <https://doi.org/10.1007/978-3-663-11385-0>.
 - [50] S. LEONARDI, *The best constant in weighted Poincaré and Friedrichs inequalities*, Rendiconti del Seminario Matematico della Università di Padova, 92 (1994), pp. 195–208.
 - [51] G. PAPANICOLAOU, A. BENSOUSSAN, AND J.-L. LIONS, *Asymptotic Analysis for Periodic Structures, Volume 5 - 1st Edition*, North Holland, 1978.
 - [52] J. SUN AND A. ZHOU, *Finite Element Methods for Eigenvalue Problems*, Chapman and Hall/CRC, 2016, <https://doi.org/10.1201/9781315372419>.
 - [53] T. A. SUSLINA, *On homogenization for a periodic elliptic operator in a strip*, St. Petersburg Math. J., 16 (2004), pp. 237–258, <https://doi.org/10.1090/S1061-0022-04-00849-0>.

- [54] L. THEISEN AND B. STAMM, *ddEigenLab.jl: Domain-Decomposition Eigenvalue Problem Lab*. Zenodo, Oct. 2021, <https://doi.org/10.5281/zenodo.5606054>.
- [55] L. THEISEN AND M. TORRILHON, *fenicsR13: A Tensorial Mixed Finite Element Solver for the Linear R13 Equations Using the FEniCS Computing Platform*, ACM Transactions on Mathematical Software, 47 (2021), pp. 17:1–17:29, <https://doi.org/10.1145/3442378>.
- [56] M. VANNINATHAN, *Homogenization of eigenvalue problems in perforated domains*, Proceedings of the Indian Academy of Sciences - Section A, 90 (1981), pp. 239–271, <https://doi.org/10.1007/BF02838079>.
- [57] K. VARGA AND J. A. DRISCOLL, *Computational Nanoscience: Applications for Molecules, Clusters, and Solids*, Cambridge University Press, Cambridge, 2011, <https://doi.org/10.1017/CBO9780511736230>.
- [58] K. B. VU, V. V. VU, H. P. THI THU, H. N. GIANG, N. M. TAM, AND S. T. NGO, *Conjugated polymers: A systematic investigation of their electronic and geometric properties using density functional theory and semi-empirical methods*, Synthetic Metals, 246 (2018), pp. 128–136, <https://doi.org/10.1016/j.synthmet.2018.10.007>.
- [59] V. V. ZHIKOV, *Weighted Sobolev spaces*, Sbornik: Mathematics, 189 (1998), pp. 1139–1170, <https://doi.org/10.1070/SM1998v189n08ABEH000344>.